

Thin and thick bubble walls II: expansion in the wall width

Ariel Mégevand* and Federico Agustín Membiela†

IFIMAR (CONICET-UNMdP)

*Departamento de Física, Facultad de Ciencias Exactas y Naturales,
UNMdP, Deán Funes 3350, (7600) Mar del Plata, Argentina*

Abstract

We study the dynamics of a cosmological bubble wall beyond the approximation of an infinitely thin wall. In a previous paper, we discussed the range of validity of this approximation and estimated the first-order corrections due to the finite width. Here, we introduce a systematic method to obtain the wall equation of motion and its profile at each order in the wall width. We discuss in detail the next-to-next-to-leading-order terms. We use the results to treat the growth of spherical bubbles and the evolution of small deformations of planar walls.

1 Introduction

The motion of bubble walls in a first-order cosmological phase transition has several consequences, such as the formation of gravitational waves [1–4] or the generation of the baryon asymmetry of the universe [5, 6]. Generally, these interfaces can be described by a field configuration in which a scalar field ϕ varies between two values corresponding to two minima of the effective potential $V(\phi)$. Such a configuration is similar to a domain wall [7]. However, in the case of a domain wall, the minima of V correspond to two true vacua, while in a phase transition the wall separates the true vacuum, which we will denote ϕ_- , from a false vacuum ϕ_+ . Therefore, for a domain wall, the potential takes the same value on both sides of the interface, while for a bubble wall we have two different values $V_- < V_+$. This pressure difference between phases is relevant to the dynamics and also affects the effective treatment of the wall as a thin interface.

Either for a bubble wall or a domain wall, it is common to use the thin-wall approximation to derive an effective equation of motion (EOM) for the wall and solve separately the equation for the wall profile. For that aim, it is usual to assume that the field only varies in the direction perpendicular to the wall hypersurface. Therefore, ϕ is a function of a single variable n . The function $\phi(n)$ describes the kink profile. On the other hand, the surface representing the wall position can be parametrized as $x^\mu = X^\mu(\xi^a)$, where

*Member of CONICET, Argentina. E-mail address: megevand@mdp.edu.ar

†Member of CONICET, Argentina. E-mail address: membiela@mdp.edu.ar

ξ^a , $a = 0, 1, 2$, are two space parameters and a time parameter. The function $X^\mu(\xi^a)$ describes the evolution of the wall as a surface.

In the case of a domain wall, the general equation for $X^\mu(\xi^a)$ has been widely discussed, even beyond the thin-wall approximation [8–19]. On the other hand, for a bubble wall, only planar, cylindrical, and spherical walls have been considered (see, e.g., [20]), as well as small perturbations of these cases [21, 22], and generally in the limit of an infinitely thin wall. A recently formed bubble is spherical, and, intuitively, the thin-wall approximation will be valid when the bubble grows and its radius R becomes much larger than the wall width l . However, a bubble wall may acquire a small radius of curvature locally due to the unstable growth of small perturbations. These can arise, for instance, from hydrodynamic instabilities [23–26] or collision with other bubbles [27–29]. More importantly, what matters is actually the curvature of the worldvolume [8, 10]. Even for a spatially planar wall, this hypersurface will curve when accelerated by a potential difference $\Delta V = V_+ - V_-$ [30]. We shall generally denote L the length scale associated to the local radius of curvature. We remark that the quantities l and L are compared in a coordinate system associated to the wall. In particular, these lengths are not Lorentz-contracted. Indeed, in the usual thin-wall approximation, the profile $\phi(n)$ is a fixed function, and its width l is a constant.

The methods used for domain walls can be adapted to bubble walls. In our previous work [30], we derived the EOM for a bubble wall of arbitrary shape and discussed the finite-width corrections. The potential difference between the minima, ΔV , introduces subtleties that make the treatment more complex. For example, the finite-width corrections for a domain wall are of order $(l/L)^2$, while for a bubble wall, there are corrections of order l/L . In the present paper, we will develop a perturbative method to obtain both the EOM and the profile at any order, and we will discuss in detail the corrections up to order $(l/L)^2$. We will consider for simplicity the case of a so-called vacuum transition, where the presence of the plasma is negligible. The method is generalizable, and in a separate paper we will incorporate the fluid into the discussion.

The plan of the paper is the following. In Sec. 2, we briefly review the basic thin-wall approximation and its shortcomings. We also introduce some tools that we will use in our analysis, such as normal Gaussian coordinates and the extrinsic curvature tensor of a hypersurface. Appendix A contains additional details. In Sec. 3, we develop our method to obtain the wall profile and EOM at any order in the wall width. In Sec. 4, we consider the wall motion for a spherical bubble and a planar wall with small deformations, and in Sec. 5 we apply the results to a specific potential. Analytic expressions for this potential as well as more general expressions can be found in App. B. In Sec. 6, we consider a convenient modification of our method to treat the $O(3,1)$ invariant solution or, equivalently, the $O(4)$ invariant instanton. Finally, in Sec. 7, we summarize our conclusions.

2 The thin-wall approximation

Since the wall is not infinitely thin, we must consider a reference surface S representing its position. For example, the set of points where ϕ takes a given value between ϕ_- and ϕ_+ . We will consider a convenient definition of this locus later. The spacetime history of the surface S constitutes a hypersurface Σ that can be represented explicitly by a parametrization $x^\mu = X^\mu(\xi^a)$. A gauge fixing is necessary to fully determine the function $X^\mu(\xi^a)$. When needed, we will use the Monge parametrization $x^3 = x_w^3(x^0, x^1, x^2)$, which

is usually appropriate for a bubble wall [30]. In this case, we have $X^\mu(\xi^a) = (\xi^a, x_w^3(\xi^a))$. We will also consider an implicit definition of the hypersurface, $F(x^\mu) = 0$. For the Monge parametrization, we have $F = x^3 - x_w^3(x^a)$. The normal vector to Σ , which satisfies the conditions $N_\mu \partial_a X^\mu = 0$ and $N_\mu N^\mu = -1$, can be defined by

$$N_\mu(x^\nu) = -\partial_\mu F / s \quad \text{with} \quad s = \sqrt{|F_{,\mu} F^{,\mu}|}. \quad (1)$$

In the Monge gauge, we have $N_\mu = (\partial_a x_w^3, -1)/s$ and $s^2 = -g^{33} + 2g^{3a} \partial_a x_w^3 - g^{ab} \partial_a x_w^3 \partial_b x_w^3$. For a vacuum transition, the equation of motion for the scalar field is

$$\nabla_\mu \nabla^\mu \phi + V'(\phi) = 0. \quad (2)$$

The basic idea of the thin-wall approximation is to obtain, from Eq. (2), an equation for the hypersurface $X^\mu(\xi^a)$, as well as an equation for the field profile $\phi(n)$, where n is a coordinate perpendicular to Σ . Since the parameters ξ^a , $a = 0, 1, 2$, represent coordinates on the worldvolume Σ , it is convenient to use the coordinates $\bar{x}^\mu = (\xi^a, n)$. In these coordinates, the field equation becomes

$$\partial_n^2 \phi - K \partial_n \phi - D_a D^a \phi = V'(\phi), \quad (3)$$

where we have defined the quantity $K = -\bar{g}^{ab} \bar{\Gamma}_{ab}^n$ and used the notation

$$D_a D^a \phi \equiv \bar{g}^{ab} (\partial_a \partial_b \phi - \bar{\Gamma}_{ab}^c \partial_c \phi). \quad (4)$$

There is not a unique way to assign coordinates ξ^a, n to points away from Σ , and we shall specifically use normal Gaussian coordinates, which are constructed as follows. We consider the set of geodesics that cross Σ perpendicularly. In a certain neighborhood of Σ , any point x^μ lies on one of these geodesics. We define the coordinate n as the distance to Σ along the geodesic. The point x^μ can be determined by n and the point $X^\mu(\xi^a)$ where the geodesic intersects Σ . We can thus assign to x^μ the new coordinates $\bar{x}^\mu = (\xi^a, n)$. Near Σ , the change of coordinates is given by the expansion

$$x^\mu = X^\mu(\xi^a) + N^\mu(\xi^a) n + \dots, \quad (5)$$

If we stay very close to Σ , this change of coordinates is equivalent to the simpler one where the expansion (5) is truncated at the linear order in n . However, normal Gaussian coordinates have good properties that are particularly useful if we go beyond that order, which is necessary when dealing with a thick wall. A few of these properties, which we will use in the next sections, are the following (see App. A for details and further expressions). The metric tensor in the coordinates $\bar{x}^\mu = (\xi^a, n)$ fulfills $\bar{g}_{nn} = -1$, $\bar{g}_{an} = 0$. In particular, this holds for the induced metric on Σ , $\gamma^{ab} = \bar{g}^{ab}|_{n=0}$. The Christoffel symbols in normal Gaussian coordinates are given by

$$\bar{\Gamma}_{nn}^\mu = \bar{\Gamma}_{\mu n}^n = 0, \quad \bar{\Gamma}_{ab}^n = \frac{1}{2} \partial_n \bar{g}_{ab}, \quad \Gamma_{na}^b = \frac{1}{2} g^{bc} \partial_n \bar{g}_{ca}. \quad (6)$$

We can invert the coordinate transformation (5) order by order to return to the original coordinates. We are only interested in the expression for $n(x^\mu)$,

$$n = \frac{F}{s} + \frac{N^\nu \partial_\nu s}{2s} \left(\frac{F}{s} \right)^2 + \left[\frac{(N^\nu \partial_\nu s)^2}{2s^2} + \frac{N^\rho N^\nu N^\mu \nabla_\rho \nabla_\nu (s N_\mu)}{6s} \right] \left(\frac{F}{s} \right)^3 + \dots \quad (7)$$

The quantity K appearing in the field equation, Eq. (3), is related to the extrinsic curvature of the hypersurfaces of $n = \text{constant}$, which we denote Σ_n . Indeed, the extrinsic curvature tensor can be defined as $K_{\mu\nu} = -\nabla_\mu n_\nu$, where n^μ is the normal vector to Σ_n , which in normal Gaussian coordinates takes the form $\bar{n}^\mu = (0, 0, 0, 1)$ (see App. A for more details). Hence, we have $\bar{K}_{n\mu} = 0$, $\bar{K}_{ab} = -\bar{\Gamma}_{ab}^n$, and

$$K = \bar{g}^{ab} \bar{K}_{ab} = g^{\mu\nu} K_{\mu\nu}. \quad (8)$$

The quantity K is sometimes called the mean curvature. In particular, at $n = 0$ we have $\Sigma_n = \Sigma$ and $n^\mu = N^\mu$. In terms of our vector field N_μ , the extrinsic curvature tensor of Σ is given by

$$K_{\mu\nu} = -h_\mu{}^\rho \nabla_\rho N_\nu. \quad (9)$$

where $h_\mu{}^\nu$ is the projection tensor orthogonal to N_μ and tangent to Σ [31],

$$h_\mu{}^\nu \equiv (\delta_\mu{}^\nu + N_\mu N^\nu). \quad (10)$$

For our perturbative treatment, we are going to need the derivatives of K evaluated at $n = 0$. We shall use the notation $K|_{n=0}$ or just $K|_0$ for $K(\xi^a, 0)$. Applying the operator $\partial_n = n^\mu \nabla_\mu$ to the previous expressions, we obtain (see App. A)

$$K|_{n=0} = -N_{;\mu}^\mu, \quad \partial_n K|_{n=0} = N_{;\nu}^\mu N_{;\mu}^\nu, \quad \partial_n^2 K|_{n=0} = -2N_{;\nu}^\mu N_{;\rho}^\nu N_{;\mu}^\rho. \quad (11)$$

The so-called thin-wall approximation actually involves a series of approximations. The first step is to assume that the field $\phi(\xi^a, n)$ only depends on the variable n (see, e.g., [7]). This assumption eliminates the derivatives tangent to the hypersurface in Eq. (3), so we have

$$\partial_n^2 \phi - K \partial_n \phi = V'(\phi). \quad (12)$$

By consistency, this equation also requires K to depend only on n [13], $K(\xi^a, n) = K(n)$. Evaluating this condition at $n = 0$ and using the expression for K from Eq. (11), we obtain an equation for the surface, namely, $N_{;\mu}^\mu = \text{constant}$. This is indeed the form of the effective EOM for the wall in the basic thin-wall approximation. However, taking the derivative of this condition, evaluating again at $n = 0$, and using the expression for $\partial_n K$ from Eq. (11), we obtain a different EOM. This shows that (except for particular cases) the assumption $\phi = \phi(n)$ must cease to hold as soon as we move away from the reference hypersurface Σ . In Ref. [30], we called the approximation $\partial_a \phi = 0$ the ‘‘incompressibility assumption’’ and argued that the error made by neglecting $\partial_a \phi$ versus $\partial_n \phi$ is

$$\frac{\partial_a \phi}{\partial_n \phi} \sim \frac{\delta l}{L} < \frac{l}{L}, \quad (13)$$

where δl represents the variations in the wall width l , while L is the local curvature radius of Σ . In [30], we argued that $\delta l \ll l$ is to be expected. Even in the case $\delta l \sim l$, the terms with derivatives with respect to ξ^a in Eq. (3) are of order $(l/L)^2$ with respect to the leading term $\partial_n^2 \phi$. We shall see that we actually have $\delta l \sim l^2$ and the term $D_a D^a \phi$ is of order $(l/L)^4$ with respect to $\partial_n^2 \phi$.

The next assumption that is usually made in the thin-wall approximation is that $K(n)$ varies little over the width of the wall, where $\partial_n \phi \neq 0$. Thus, multiplying Eq. (12) by $\partial_n \phi$ and integrating from $n = -\infty$ to $n = +\infty$, we obtain

$$K = -\Delta V / \sigma, \quad (14)$$

where $\Delta V = V_+ - V_-$ with $V_{\pm} = V(\phi_{\pm})$, and $\sigma = \int_{-\infty}^{+\infty} (\partial_n \phi)^2 dn$ is the surface tension. Using Eq. (11), we obtain an equation for the normal vector, $N^{\mu}_{;\mu} = \Delta V / \sigma$. Using Eq. (1) with the Monge parametrization, we obtain an equation for the wall position $x_w^3(x^0, x^1, x^2)$. This equation depends on the chosen coordinates and we will discuss it in Sec. 4. From a geometric point of view, the meaning of Eq. (14) is that the potential difference causes an acceleration and, therefore, curves the hypersurface.

To obtain the value of σ , we need to solve the equation for ϕ , Eq. (12), which depends on K and, hence, on σ . Therefore, it is usual to make yet another approximation, which consists in neglecting the second term in Eq. (12) since it is of order l/L with respect to the first one. The resulting equation, $\partial_n^2 \phi = V'(\phi)$, is readily integrated. Imposing the condition $\phi(+\infty) = \phi_+$, we obtain

$$\phi'^2 = 2(V - V_+). \quad (15)$$

If we evaluate this equation at $n = -\infty$, we obtain $\Delta V = 0$. This means that this approximation requires, for consistency, a potential with $V_+ = V_-$. This looks incompatible with Eq. (14), but here we have made an extra approximation to estimate the parameter σ . In any case, as discussed in [30], the approximation of small l/L may break down since Eq. (14) introduces a curvature radius L which is naturally of order l unless ΔV is relatively small. Specifically, for a planar wall we roughly have $l/L \sim \Delta V / V_b$, where V_b is the height of the barrier between the minima of the potential¹ (additionally, the wall may be curved even for $\Delta V = 0$).

To implement the approximation of a small ΔV , it is convenient to write V in the form [32]

$$V(\phi) = V_0(\phi) + \tilde{V}(\phi), \quad (16)$$

where V_0 is a degenerate potential and \tilde{V} causes the energy difference between minima. The decomposition (16) is not unique and a convenient form for \tilde{V} can be chosen (e.g., a linear term $\tilde{V} = c\phi$ or a quadratic term $\tilde{V} = \frac{1}{2}\delta m^2 \phi^2$). Then, we define $V_0 = V - \tilde{V}$ and we choose the parameters in \tilde{V} so that the minima of V_0 have the same energy. Denoting these minima a_{\pm} , we have the conditions [30]

$$\tilde{V}'(a_{\pm}) = V'(a_{\pm}), \quad (17)$$

$$\tilde{V}(a_+) - \tilde{V}(a_-) = V(a_+) - V(a_-). \quad (18)$$

If \tilde{V} contains a single free parameter, these equations determine its value, which will be of the order of ΔV . Using the approximation $V \simeq V_0$, Eq. (15) can be easily solved, and from the profile $\phi(n)$ we obtain the surface tension σ . Using this value in Eq. (14), we obtain a closed equation for the wall surface. It is worth remarking that this equation of motion for the wall and the equation for the profile, Eq. (15), were both derived from Eq. (12). However, in Eq. (14), the leading-order term $\partial_n^2 \phi$ vanished upon integration, so the whole equation (14) is of higher order. In contrast, Eq. (15) retains this term and neglects the second one in Eq. (12), which, according to Eq. (14), is proportional to ΔV . This is why Eq. (15) is consistent with $\Delta V = 0$.

¹This estimation is valid for a nearly degenerate potential [30], where the barrier height can be unambiguously defined as the difference between the maximum of the potential and any of the minima, and we have $\Delta V \ll V_b$. In Sec. 5, we will use the ratio $\Delta V / V_b$ to characterize the shape of the potential even when this condition is not fulfilled. We will use the definition $V_b = V(\phi_b) - V_+$, where ϕ_b is the value of ϕ at the maximum.

3 The perturbative expansion

To go beyond the above approximations, let us consider the first integral of Eq. (3),

$$\frac{1}{2}(\partial_n\phi)^2 + \int_n^\infty [K(\partial_n\phi)^2 + \partial_n\phi D_a D^a\phi] d\tilde{n} = -[V_+ - V(\phi)], \quad (19)$$

which is obtained by multiplying the equation by $\partial_n\phi$ and integrating through the wall. We have imposed the condition $\phi(+\infty) = \phi_+$. We also assume that $\phi(-\infty) = \phi_-$, so, evaluating Eq. (19) at $n = -\infty$, we have

$$\int_{-\infty}^{+\infty} [(\partial_n\phi)^2 K + \partial_n\phi D_a D^a\phi] dn = -\Delta V. \quad (20)$$

As we will see below, these equations are the generalization of Eqs. (14) and (15) to all order in the wall width. We have not yet given a precise definition of the reference surface S associated to the wall position, whose worldvolume is given by the hypersurface Σ located at $n = 0$. Taking into account that the energy density of the wall is proportional to the quantity $(\partial_n\phi)^2$, it makes sense to define the wall position as the average of n weighted with this quantity. Since, by definition, the wall position is $n = 0$, we have

$$\int_{-\infty}^{+\infty} (\partial_n\phi)^2 n dn = 0. \quad (21)$$

This condition will fix an integration constant in the solution of Eq. (19). We can also define the wall width l as the root mean square value of n , i.e.,

$$l^2 = \frac{\int_{-\infty}^{+\infty} (\partial_n\phi)^2 n^2 dn}{\int_{-\infty}^{+\infty} (\partial_n\phi)^2 dn} \equiv \frac{\mu}{\sigma}, \quad (22)$$

where $\sigma = \int_{-\infty}^{+\infty} (\partial_n\phi)^2 dn$ is the surface tension and we have also defined the quantity $\mu = \int_{-\infty}^{+\infty} (\partial_n\phi)^2 n^2 dn$, which will appear below.

Let us denote ϕ_0 the solution obtained from Eq. (3) or its first integral (19) with the approximations used in the previous section, namely, $D_a D^a\phi = 0$, $K = 0$, and $V = V_0$. Thus, Eq. (3) becomes

$$\phi_0''(n) = V_0'(\phi_0) \quad (23)$$

and Eq. (19) becomes $\phi_0'^2 = 2(V_0 - V_{0+})$, which is the usual thin-wall equation for the profile, Eq. (15), with V replaced by V_0 and V_+ by $V_{0+} \equiv V_0(a_+)$, i.e., for consistency, ϕ_0 must fulfill the boundary conditions $\phi_0(\pm\infty) = a_\pm$ (the minima of V_0). We regard this equation as the leading-order version of Eq. (19). We thus have

$$\phi_0'(n) = -\sqrt{2[V_0(\phi_0) - V_0(a_+)]} \equiv -\phi_h(\phi_0), \quad (24)$$

where the sign chosen for the square root corresponds to assuming $a_+ < a_-$. Integrating Eq. (24), we obtain the implicit solution

$$n = -\int_{\phi_*}^{\phi_0} \frac{d\phi}{\phi_h(\phi)} + n_*. \quad (25)$$

The value ϕ_* is arbitrary, and we determine the constant n_* by imposing the condition (21) to ϕ_0 . We obtain

$$n_* = \sigma_0^{-1} \int_{a_+}^{a_-} d\phi_0 \left[\phi_h(\phi_0) \int_{\phi_*}^{\phi_0} \frac{d\phi}{\phi_h(\phi)} \right], \quad (26)$$

with $\sigma_0 = \int_{-\infty}^{+\infty} (\partial_n \phi_0)^2 dn$. Notice that using the same approximations in Eq. (20) just gives $0 = 0$. Nevertheless, at the next order we will obtain the leading-order equation for the wall, Eq. (14).

To obtain the field profile and the wall EOM at higher orders in the wall width, we need to take into account that the quantities K , $D_a D^a \phi$, and $V - V_0$ do not vanish. We begin by writing the field in the form

$$\phi = \phi_0 + \phi_1 + \phi_2 + \dots, \quad (27)$$

where each term is of order l/L higher than the previous one. The concrete definition of each term ϕ_i is that the sum (27) up to each order i gives the solution to Eq. (19) to that order. In particular, ϕ_0 is the solution of Eq. (24). These solutions will include the boundary conditions at each order, $\phi(\pm\infty) = \phi_{\pm}$, so we write

$$\phi_{\pm} = a_{\pm} + \phi_{1\pm} + \phi_{2\pm} + \dots. \quad (28)$$

Taking into account that the term \tilde{V} in Eq. (16) is of order l/L and expanding V in powers of $\phi - \phi_0$, we have

$$V(\phi) = V_0(\phi_0) + [\tilde{V}(\phi_0) + V_0'(\phi_0)\phi_1] + [\tilde{V}'(\phi_0)\phi_1 + \frac{1}{2}V_0''(\phi_0)\phi_1^2 + V_0'(\phi_0)\phi_2] + \dots, \quad (29)$$

where we have grouped terms of the same order in l/L . In particular, evaluating this expression at the minima, we obtain $V_{\pm} = V_{0\pm} + V_{1\pm} + \dots$, with

$$V_{0\pm} = V_0(a_{\pm}), \quad V_{1\pm} = \tilde{V}(a_{\pm}), \quad V_{2\pm} = \tilde{V}'(a_{\pm})\phi_{1\pm} + \frac{1}{2}V_0''(a_{\pm})\phi_{1\pm}^2 \quad (30)$$

$$V_{3\pm} = \frac{1}{2}\tilde{V}''(a_{\pm})\phi_{1\pm}^2 + \frac{1}{6}V_0'''(a_{\pm})\phi_{1\pm}^3 + V_0''(a_{\pm})\phi_{1\pm}\phi_{2\pm} + \tilde{V}'(a_{\pm})\phi_{2\pm}, \dots \quad (31)$$

and $\Delta V = \Delta V_1 + \dots$, with $\Delta V_i = V_{i+} - V_{i-}$.

In Sec. 2, we considered two different approximations for the quantity K , namely, that it can be neglected, and that its variation can be neglected. We must regard these as approximations of different order in the wall width. First of all, let us write

$$K = K_0 + K_1 + K_2 + \dots, \quad (32)$$

where each term is of order l/L higher than the previous one. Unlike ϕ , K does not have a significant variation within the width of the wall, so we can use its expansion as a Taylor series in n . We consider such an expansion for each term in Eq. (32),

$$K_i = K_i|_{n=0} + \partial_n K_i|_{n=0} n + \frac{1}{2}\partial_n^2 K_i|_{n=0} n^2 + \dots, \quad (33)$$

It is important to note that the subscripts in the expansions (27)-(33) only indicate the relative order of a term within the quantity being expanded. We need to insert these expansions in Eqs. (19)-(20) and compare the terms. Each of the above quantities

scales with different powers of l and L , and, besides, there are derivatives and integrals in Eqs. (19)-(20). To assess the absolute order of a term, we must take into account, in the first place, that the order of magnitude of both ϕ and l is given by the scale of the theory v as $\phi \sim v$, $l \sim v^{-1}$. This means that we have $\phi_0 \sim l^{-1}$, $\phi_1 \sim l^{-1}(l/L) = L^{-1}$, $\phi_2 \sim lL^{-2}$, and so on. In the second place, the mean curvature K is (by definition of L) of order L^{-1} , so we have $K_0 \sim L^{-1}$, $K_1 \sim L^{-1}(l/L) = lL^{-2}$, and so on. In the third place, a derivative ∂_n applied to ϕ_i changes the order by a factor l^{-1} , but applied to K changes the order by L^{-1} . On the other hand, the operator $D_a D^a$ is of order L^{-2} . Finally, we must take into account that the integral increases the order by a factor l , since the integrand vanishes outside the wall. For the same reason, each power of n increases the order by a factor l . The lowest-order terms in Eq. (19) are of order l^{-4} . Retaining only these terms, we obtain Eq. (24). The terms of order i are those of order $l^{-4}(l/L)^i$.

When we insert the expansion (32)-(33) in Eqs. (19) and (20), the integral of $K(\partial_n \phi)^2$ will split into a combination of integrals of the form

$$I^{(k)}(\xi^a, n) = \int_n^\infty (\partial_n \phi)^2 \tilde{n}^k d\tilde{n}, \quad \bar{I}^{(k)}(\xi^a) = \int_{-\infty}^{+\infty} (\partial_n \phi)^2 n^k dn. \quad (34)$$

Thus, we have $I^{(k)}|_{n=+\infty} = 0$ and $I^{(k)}|_{n=-\infty} = \bar{I}^{(k)}$. In particular, for $k = 0, 1, 2$, we obtain the integrals appearing in Eqs. (21)-(22), so we have $\sigma = \bar{I}^{(0)}$, $\mu = \bar{I}^{(2)}$, and the condition $\bar{I}^{(1)} = 0$.² When we insert the expansion (27) in the quantities (34), we will have, at each order in l/L , integrals of the form

$$I_0^{(k)} = \int_n^\infty (\partial_n \phi_0)^2 \tilde{n}^k d\tilde{n}, \quad I_1^{(k)} = \int_n^\infty 2\partial_n \phi_0 \partial_n \phi_1 \tilde{n}^k d\tilde{n}, \quad I_2^{(k)} = \int_n^\infty [(\partial_n \phi_1)^2 + 2\partial_n \phi_0 \partial_n \phi_2] \tilde{n}^k d\tilde{n}, \quad (35)$$

and so on, as well as definite integrals $\bar{I}_i^{(k)}$. In particular, we have $\bar{I}_i^{(0)}| = \sigma_i$ and $\bar{I}_i^{(2)} = \mu_i$, where σ_i and μ_i are the terms of the expansion of σ and μ at successive orders in l/L .

Expanding Eq. (19) to order i and taking into account that the field ϕ_{i-1} fulfills the equation for the previous order, we obtain the equation for ϕ_i ,

$$\partial_n \phi_0 \partial_n \phi_i - \partial_n^2 \phi_0 \phi_i = f_i, \quad (36)$$

where we have also used Eq. (23). The first few functions f_i are given by

$$f_1 = \tilde{V}(\phi_0) - V_{1+} - K_0|_0 I_0^{(0)}, \quad (37)$$

$$f_2 = \tilde{V}'(\phi_0) \phi_1 + \frac{1}{2} V_0''(\phi_0) \phi_1^2 - V_{2+} - \frac{1}{2} (\partial_n \phi_1)^2 - K_0|_0 I_1^{(0)} - K_1|_0 I_0^{(0)} - \partial_n K_0|_0 I_0^{(1)}, \quad (38)$$

$$f_3 = \tilde{V}'(\phi_0) \phi_2 + \frac{1}{2} \tilde{V}''(\phi_0) \phi_1^2 + V_0''(\phi_0) \phi_1 \phi_2 + \frac{1}{6} V_0'''(\phi_0) \phi_1^3 - V_{3+} - \partial_n \phi_1 \partial_n \phi_2 - K_0|_0 I_2^{(0)} - K_1|_0 I_1^{(0)} - K_2|_0 I_0^{(0)} - \partial_n K_0|_0 I_1^{(1)} - \partial_n K_1|_0 I_0^{(1)} - \frac{1}{2} \partial_n^2 K_0|_0 I_0^{(2)}. \quad (39)$$

Similarly, expanding Eq. (20), we will obtain the equations for the quantities $K_i|_0$. Instead of repeating the procedure, we may, equivalently, evaluate Eqs. (36) at $n = -\infty$, which gives $f_i|_{n=-\infty} = 0$. Therefore, Eqs. (37)-(39) give

$$K_0|_{n=0} \sigma_0 = -\Delta V_1, \quad (40)$$

$$K_0|_{n=0} \sigma_1 + K_1|_{n=0} \sigma_0 = -\Delta V_2, \quad (41)$$

$$\sigma_2 K_0|_{n=0} + \sigma_1 K_1|_{n=0} + \sigma_0 K_2|_{n=0} + (\mu_0/2) (\partial_n^2 K_0)|_{n=0} = -\Delta V_3. \quad (42)$$

²Since $\bar{I}^{(1)} = 0$ and $\partial_n I^{(1)} = -n(\partial_n \phi)^2$, an integration by parts gives the relation $\int_{-\infty}^{+\infty} I^{(1)} n^j dn = \frac{1}{j+1} \bar{I}^{(j+2)}$, which can be used to obtain some of the results we give below.

The quantity $K|_0$ at lowest non-trivial order is given by Eq. (40), and we obtain the usual equation of motion for the wall, Eq. (14). We remark that the parameter σ_0 and, hence, the quantity $K_0|_0$, involves the field profile ϕ_0 obtained from the previous-order equation (24). Therefore, the function f_1 only depends on the previous solution ϕ_0 , and is a source term in the equation for ϕ_1 . Notice also that f_1 is only a function of n , so Eq. (36) gives a solution of the form $\phi_1 = \phi_1(n)$. The term containing $D_a D^a \phi$ in Eqs. (19)-(20) has not appeared in Eqs.(37)-(42) because it vanishes at these low orders. Indeed, its lowest-order terms $D_a D^a \phi_0$, $D_a D^a \phi_1$, would appear in the quantities f_2 and f_3 , but these terms vanish since ϕ_0 and ϕ_1 do not depend on ξ^a .

To solve the system of differential equations (36), we only need to note that the i -th function f_i depends only on the previous solutions $\phi_0, \dots, \phi_{i-1}$. Once these are solved, the equation for ϕ_i is just a first order non-homogeneous differential equation in the variable n . The homogeneous equation is the same for every i , namely, $\phi'_0 \partial_n \phi_i - \phi''_0 \phi_i = 0$, whose general solution is proportional to the function ϕ_h defined in Eq. (24). The general solution of the non-homogeneous equation can be obtained, e.g., by variation of constants, and is given by

$$\phi_i(\xi^a, n) = \phi_h(n) [C_i(\xi^a, n) + c_i(\xi^a)], \quad (43)$$

where the function C_i is given by

$$C_i(\xi^a, n) = - \int_{n_*}^n \frac{f_i(\tilde{n}, \xi^a)}{\phi_h(\tilde{n})^2} d\tilde{n}, \quad (44)$$

and c_i is a constant of integration (with respect to n), which must be determined by imposing the condition (21) at each order, i.e., $\bar{I}_i^{(1)} = 0$. Integrating by parts in Eq. (35) and replacing (43), we obtain, for $i = 1, 2$,

$$c_1 = -2\sigma_0^{-1} \int_{-\infty}^{+\infty} [\phi'_0 + n\phi''_0] \phi'_0 C_1 dn, \quad (45)$$

$$c_2 = -\sigma_0^{-1} \int_{-\infty}^{+\infty} [2(n\phi''_0 + \phi'_0) \phi'_0 C_2 + \phi_1'^2 n] dn. \quad (46)$$

While the function f_1 only depends on n , the function f_2 can depend on ξ^a since the quantity $\partial_n K_0|_0$ in Eq. (38) can depend on the point of Σ . Therefore, the field ϕ_2 will generally depend on ξ^a . It is convenient to single out the ξ^a -dependent term in the expressions. Hence, we write

$$f_2(\xi^a, n) = \tilde{f}_2(n) - I_0^{(1)}(n) \partial_n K_0(\xi^a, 0) \quad (47)$$

and $C_2 = C_{2a} + C_{2b} \partial_n K_0|_{n=0}$, where

$$C_{2a}(n) = \int_{n_*}^n \frac{\tilde{f}_2(\tilde{n})}{\phi_h(\tilde{n})^2} d\tilde{n}, \quad C_{2b}(n) = - \int_{n_*}^n \frac{I_0^{(1)}(\tilde{n})}{\phi_h(\tilde{n})^2} d\tilde{n}. \quad (48)$$

We also define

$$c_{2a} = -\sigma_0^{-1} \int_{-\infty}^{+\infty} [2(n\phi''_0 + \phi'_0) \phi'_0 C_{2a} + \phi_1'^2 n] dn, \quad c_{2b} = -\sigma_0^{-1} \int_{-\infty}^{+\infty} 2(n\phi''_0 + \phi'_0) \phi'_0 C_{2b} dn, \quad (49)$$

so that we can write $\phi_2(\xi^a, n) = \phi_{2a}(n) + \phi_{2b}(n)\partial_n K_0(\xi^a, 0)$. The complete wall profile up to next-to-next-to-leading order is given by

$$\phi(\xi^a, n) = \phi_0(n) + \phi_1(n) + \phi_{2a}(n) + \phi_{2b}(n)\partial_n K_0(\xi^a, 0). \quad (50)$$

To change from the coordinates ξ^a, n to the original coordinates x^μ , we can use Eq. (7) to obtain $n(x^\mu)$, while Eq. (11) gives the quantity $\partial_n K|_0$ as a scalar in terms of N^μ , and we can readily write it in any coordinates.

To solve for the quantity $K|_{n=0}$ at each order, we first obtain, from Eq. (40),

$$K_0|_{n=0} = -\Delta V_1/\sigma_0. \quad (51)$$

Using Eq. (51) in Eq. (41), we can solve for $K_1|_0$,

$$K_1|_{n=0} = -\Delta V_2/\sigma_0 + \Delta V_1\sigma_1/\sigma_0^2. \quad (52)$$

The quantity σ_1 depends on the solution $\phi_1(n)$ and is a constant, so the first correction to $K|_0$ is a constant too. Using Eq. (36) in the second of Eqs. (35), we obtain $\sigma_1 = \int_{-\infty}^{+\infty} f_1(n)dn$. Finally, using Eqs. (51) and (52) in Eq. (42), we solve for $K_2|_0$,

$$K_2|_{n=0} = \Delta V_1\sigma_2/\sigma_0^2 - \Delta V_1\sigma_1^2/\sigma_0^3 + \Delta V_2\sigma_1/\sigma_0^2 - \Delta V_3/\sigma_0 - (\mu_0/2\sigma_0)\partial_n^2 K_0|_{n=0}. \quad (53)$$

This correction to K will not be a constant in general, since the quantities σ_2 and $\partial_n^2 K_0|_0$ may depend on ξ^a . Using Eq. (36) in the third of Eqs. (35), the separation (47) gives

$$\sigma_2 = \tilde{\sigma}_2 - \mu_0\partial_n K_0(\xi^a, 0), \quad (54)$$

where the quantities $\tilde{\sigma}_2 = \int_{-\infty}^{+\infty} (\phi_1'^2 + \tilde{f}_2)dn$ and $\mu_0 = \int_{-\infty}^{+\infty} \phi_0'^2 n^2 dn$ are constants.

Using Eqs. (11), we can write Eqs. (51)-(54) in terms of the normal vector N^μ . Thus, Eq. (51) becomes $N_{0;\mu}^\mu = \Delta V_1/\sigma_0$. This is the leading-order (LO) equation for the hypersurface and is equivalent to Eq. (14). If we are satisfied with the lowest order, we can replace the value ΔV_1 with ΔV , since the difference is of higher order. Thus, we can write

$$N_{0;\mu}^\mu = \Delta V/\sigma_0. \quad (55)$$

For the first correction to the normal vector, Eq. (52) gives an equation of the same form, namely, $N_{1;\mu}^\mu = \text{constant}$. Alternatively, we can obtain an equation for the full N^μ to this order. Indeed, if we add Eqs. (40) and (41), the expression on the left-hand side is the expansion of $\sigma K|_0$, while on the right-hand side we have the expansion of ΔV , both to next-to-leading order (NLO) in l/L . Therefore, if we only need results to this order, we may write $K|_0 = -\Delta V/\sigma$, where $\sigma = \sigma_0 + \sigma_1$. Thus, the equation is the same as the lowest-order one, only with the parameter σ updated,

$$N_{;\mu}^\mu = \Delta V/\sigma. \quad (56)$$

Similarly, from Eq. (53) we obtain an equation for N_2^μ , but we can also add Eqs. (40)-(42) and identify the expansions of $\sigma K|_{n=0}$ and ΔV up to the next-to-next-to-leading order (NNLO), to obtain an equation for the full N^μ up to this order,

$$\sigma K|_{n=0} = -\Delta V - (\mu_0/2)\partial_n^2 K_0|_{n=0}. \quad (57)$$

We see that the wall EOM is no longer of the form $N^\mu{}_{;\mu} = \Delta V/\sigma$. Moreover, the quantity σ is not a constant at this order, and this fact should be taken into account explicitly in the equation for N^μ . Using the separation (54) and defining the parameter $\tilde{\sigma} = \sigma_0 + \sigma_1 + \tilde{\sigma}_2$, we may write Eq. (57) as

$$\tilde{\sigma}K|_{n=0} - \mu_0(K_0\partial_n K_0)|_{n=0} + (\mu_0/2)\partial_n^2 K_0|_{n=0} = -\Delta V. \quad (58)$$

We could actually replace K_0 by K everywhere, since μ_0 is of order l^2 . Thus, we would obtain an equation for the full quantity $K(\xi^a, 0)$ to this order. Then, using Eqs. (11) for K and its derivatives, we have an equation for N^μ . However, solving this equation can be cumbersome since the second and third terms in (58) are non-linear in N^μ . In most cases, it will be more pragmatic to just keep K to leading order in the terms proportional to μ_0 . Moreover, in these terms we can use the approximation $\tilde{\sigma} = \sigma_0$. Using also the LO equation $K_0|_0 = -\Delta V/\sigma_0$, we obtain, in terms of N^μ ,

$$N^\mu{}_{;\mu} = \frac{\Delta V}{\tilde{\sigma}} + \frac{\mu_0}{\sigma_0} \left(\frac{\Delta V}{\sigma_0} N^\mu{}_{0;\nu} N^\nu{}_{0;\mu} - N^\mu{}_{0;\nu} N^\nu{}_{0;\rho} N^\rho{}_{0;\mu} \right). \quad (59)$$

The left-hand side of Eq. (59) is like in the previous orders, while the right-hand side contains source terms which depend on the leading-order solution. The only vestige of the NLO correction is the term σ_1 in the quantity $\tilde{\sigma}$.

For a domain wall (i.e., in the case $\Delta V = 0$), the LO and NLO equations are exactly the same, namely, $N^\mu{}_{;\mu} = 0$, while the NNLO equation is $N^\mu{}_{;\mu} = -(\mu_0/\sigma_0)N^\mu{}_{0;\nu}N^\nu{}_{0;\rho}N^\rho{}_{0;\mu}$. This result is in agreement with Ref. [10], where it was obtained using an iterative process (see also [11, 13, 14, 16, 17] for similar calculations). In this case, we have $\tilde{V} = 0$ and $K_0|_0 = 0$, which give $f_1 = 0$, and, hence, $\phi_1 = 0$, i.e., there is no correction to the wall profile at this order. Since we have $K_1|_0 = 0$, we obtain $\tilde{f}_2 = 0$, which implies $\phi_2 = \phi_{2b}(n)\partial_n K_0(\xi^a, 0)$.

To put the wall EOM in terms of the wall position $X^a(\xi^a)$, we shall use the Monge parametrization $x^3 = x_w^3(x^0, x^1, x^2)$ and replace $N_\mu = (\partial_a x_w^3, -1)/s$ in the above results. We can proceed in different ways. For instance, writing $x_w^3 = x_{w0}^3 + x_{w1}^3 + \dots$, we may obtain an equation for each term x_{wi}^3 from Eqs. (51)-(53) and solve order by order. This method will give nonlinear equations due to the normalization factor $1/s$. An alternative is to complete an equation for the full quantity N^μ up to the highest order under consideration, as discussed below Eq. (58). This gives an equation for a single function x_w^3 . Such an equation will contain non-linear terms, but will be particularly useful for treating linearized perturbations such a small deformations from a planar or spherical wall. Another possibility is to solve the EOM for x_w^3 up to a given order and then use the solution as a source term in the next-order EOM, as in the sequence of equations (55), (56), (59). Let us consider this recursive approach.

In Ref. [30] we wrote the LO and NLO equations for x_w^3 (which have the same form) without specifying a particular coordinate system. Beyond the next-to-leading order, such general expressions become very cumbersome. In Minkowski space and using Cartesian coordinates $x^a = t, x, y, x^3 = z$ with the metric $\eta_{\mu\nu} = \text{diag}(1, -1, -1, -1)$, we have the parametrization $z = z_w(t, x, y)$, and the leading-order EOM, Eq. (55), becomes

$$\partial_a \frac{\partial^a z_{w0}}{s_0} = \frac{\Delta V}{\sigma_0}, \quad (60)$$

with $s_0 = \sqrt{1 - \partial_c z_{w0} \partial^c z_{w0}}$. The NLO EOM, Eq. (56), takes the same form, with the parameter σ_0 replaced by $\sigma_0 + \sigma_1$. Using the relation $l_0^2 = \mu_0/\sigma_0$ [from Eq. (22)], the NNLO EOM, Eq. (59), becomes

$$\partial_a \frac{\partial^a z_w}{s} = \frac{\Delta V}{\tilde{\sigma}} + l_0^2 \frac{\Delta V}{\sigma_0} \partial_b \frac{\partial^a z_{w0}}{s_0} \partial_a \frac{\partial^b z_{w0}}{s_0} - l_0^2 \partial_b \frac{\partial^a z_{w0}}{s_0} \partial_c \frac{\partial^b z_{w0}}{s_0} \partial_a \frac{\partial^c z_{w0}}{s_0}, \quad (61)$$

with $s = \sqrt{1 - \partial_a z_w \partial^a z_w}$. These equations of motion are still general, but are most useful to treat deformations of a planar wall. In Sec. 4 we consider spherical coordinates for the case of a spherically symmetric bubble.

Finally, let us consider the surface tension and the wall width. Using Eq. (54), the former can be written in the form $\sigma = \tilde{\sigma} + \delta\sigma(\xi^a)$, with

$$\tilde{\sigma} = \sigma_0 + \sigma_1 + \tilde{\sigma}_2, \quad \delta\sigma = -\mu_0 \partial_n K_0|_0, \quad (62)$$

On the other hand, the definition (22) gives $l_0 = \sqrt{\mu_0/\sigma_0}$. To obtain l to higher orders, we will need the expansion of μ . Proceeding like we did for σ , we obtain

$$\mu_1 = \int_{-\infty}^{+\infty} (f_1 n^2 + 2\phi_0'^2 C_1 n) dn \quad (63)$$

and $\mu_2 = \tilde{\mu}_2 + \alpha \partial_n K_0(\xi^a, 0)$, with

$$\tilde{\mu}_2 = \int_{-\infty}^{+\infty} [(\phi_1'^2 + \tilde{f}_2) n^2 + 2\phi_0'^2 C_{2a} n] dn, \quad \alpha = \int_{-\infty}^{+\infty} (2C_{2b} n - \frac{1}{3} n^4) \phi_0'^2 dn. \quad (64)$$

Therefore, Eq. (22) gives $l = \tilde{l} + \delta l(\xi^a)$, with

$$\tilde{l} = l_0 \left[1 + \frac{1}{2} \frac{\mu_1}{\mu_0} - \frac{1}{2} \frac{\sigma_1}{\sigma_0} - \frac{1}{8} \frac{\mu_1^2}{\mu_0^2} + \frac{3}{8} \frac{\sigma_1^2}{\sigma_0^2} - \frac{1}{4} \frac{\sigma_1 \mu_1}{\sigma_0 \mu_0} + \frac{1}{2} \frac{\tilde{\mu}_2}{\mu_0} - \frac{1}{2} \frac{\tilde{\sigma}_2}{\sigma_0} \right], \quad (65)$$

$$\delta l = \frac{l_0}{2} \left[\frac{\alpha}{\mu_0} + \frac{\mu_0}{\sigma_0} \right] \partial_n K_0|_0. \quad (66)$$

These quantities may depend on the point of the hypersurface through the quantity $\partial_n K_0$, which is given by Eq. (11). We have

$$\partial_n K_0|_0 = \partial_b \frac{\partial^a z_{w0}}{s_0} \partial_a \frac{\partial^b z_{w0}}{s_0}. \quad (67)$$

This quantity also appears in the expression for the field profile, Eq. (50). The latter depends also on the variable n , which is given by Eq. (7). We have

$$n = \frac{z - z_w}{s} - \frac{\partial^c z_w \partial^b z_w \partial_b \partial_c z_w (z - z_w)^2}{2s^3} \frac{1}{s^2} + \left[\frac{(\partial^c z_w \partial^b z_w \partial_b \partial_c z_w)^2}{2s^6} + \frac{\partial^a z_w \partial^b z_w \partial^c z_w \partial_b \partial_c \partial_a z_w}{6s^4} \right] \frac{(z - z_w)^3}{s^3} + \dots \quad (68)$$

4 The wall motion

We will use Eq. (61) to study the evolution of a planar wall and deformations thereof. It is worth emphasizing that this EOM makes no assumptions about the shape of the wall, and is valid as long as the parametrization $z = z_w(t, x, y)$ holds, which is always possible locally. A similar but more cumbersome equation can be obtained in spherical coordinates (see our previous work [30] for the leading-order equation), which will be more appropriate for a realistic bubble. For the case of a spherical wall without deformations, we will derive the EOM directly from Eq. (59).

4.1 Planar wall

The evolution of a spatially-planar wall is equivalent to a 1+1 dimensional problem. We have $z_w(t, x, y) = z_w(t)$, $s = \sqrt{1 - \dot{z}_w^2} = \gamma_w^{-1}$, and Eqs. (60)-(61) become

$$\gamma_{w0}^3 \ddot{z}_{w0} = \Delta V / \sigma_0, \quad (69)$$

$$\gamma_w^3 \ddot{z}_w = \frac{\Delta V}{\tilde{\sigma}} + l_0^2 \frac{\Delta V}{\sigma_0} (\gamma_{w0}^3 \ddot{z}_{w0})^2 - l_0^2 (\gamma_{w0}^3 \ddot{z}_{w0})^3. \quad (70)$$

Inserting the former in the latter, we obtain

$$\gamma_w^3 \ddot{z}_w = \Delta V / \tilde{\sigma}. \quad (71)$$

In the case of a domain wall, with $\Delta V = 0$, this equation is just $\ddot{z}_w = 0$, as expected. For $\Delta V \neq 0$, the NNLO equation has the same form as the LO one, with the replacement $\sigma_0 \rightarrow \tilde{\sigma}$. The EOM also gives the mean curvature of the hypersurface, and in this case we have $K = -\gamma_w^3 \ddot{z}_w = \text{constant}$. Therefore, we define the parameter $L \equiv |K|^{-1}$ associated to the curvature radius³. At leading order we have $L_0 = \sigma_0 / \Delta V$ and at next-to-next-to-leading order we have $L = \tilde{\sigma} / \Delta V$. We remark that $\tilde{\sigma}$ is not the total NNLO surface tension, which is given by Eq. (62) as $\sigma = \tilde{\sigma} + \delta\sigma$. In the present case, we have $\delta\sigma = -\sigma_0 l_0^2 / L_0^2$, but this contribution disappears from K as the last two terms in Eq. (70) cancel each other out.

The leading-order EOM, Eq. (69), has the first integral $\gamma_{w0} - \gamma_{i0} = (z_{w0} - z_{i0}) / L_0$, where z_{i0}, γ_{i0} are the initial values. It is straightforward to solve algebraically for \dot{z}_{w0} and then integrate the first-order differential equation. We obtain

$$z_{w0} = z_{i0} - L_0 \gamma_{i0} + \sqrt{L_0^2 + (t + L_0 \gamma_{i0} \dot{z}_{i0})^2}. \quad (72)$$

Similarly, we have $\gamma_w = \gamma_i + (z_w - z_i) / L$ and

$$z_w = z_i - L \gamma_i + \sqrt{L^2 + (t + L \gamma_i \dot{z}_i)^2}. \quad (73)$$

The initial conditions depend on the problem under consideration and can be different at each order. In the specific case of a vacuum phase transition in 1+1 dimensions, z_i

³Since $K = \gamma^{ab} K_{ab}$ is the the trace of the extrinsic curvature tensor, for a three-dimensional hypersurface we have $K = k_1 + k_2 + k_3$, where the eigenvalues k_i give the principal curvatures [33, 34], and we may define the corresponding curvature radii $L_i = |k_i|^{-1}$. For a spatially planar wall, we have $K_{\mu\nu} = -(\delta_\mu^0 \delta_\nu^0 - \delta_\mu^z \delta_\nu^z \dot{z}_w - \delta_\mu^z \delta_\nu^0 \dot{z}_w + \delta_\mu^z \delta_\nu^z \dot{z}_w^2) \gamma_w^5 \ddot{z}_w$, and there is only one non-vanishing eigenvalue, $k_1 = -\gamma_w^3 \ddot{z}_w$, with eigenvector $\gamma_w(1, 0, 0, -\dot{z}_w)$.

corresponds to the bubble radius at nucleation. For consistency, in that case z_i should be calculated using the thin-wall approximation for the instanton to the corresponding order. We discuss such a calculation in Sec. 6. On the other hand, if we just want to describe the evolution of a planar wall from a given initial condition, then we should use the same value of z_i at each order.

Writing Eq. (73) in the form $(z_w - z_i + L\gamma_i)^2 = L^2 + (t + L\gamma_i\dot{z}_i)^2$, we see that the solution is invariant under Lorentz transformations. This is more apparent if we translate the origin of the coordinate system to the point $t_0 = -L\gamma_i\dot{z}_i$, $z_0 = z_i - L\gamma_i$, so that the new initial values are $z_i = L$, $\dot{z}_i = 0$ and we have $\gamma_w = z_w/L$ and $z_w^2 = L^2 + t^2$. This result is in agreement with the existence of a Lorentz-invariant solution of Eq. (2) for $\phi(z, t)$.

Using the above expressions in Eqs. (67) and (68), we obtain the quantities $\partial_n K_0|_0 = (\Delta V/\sigma_0)^2$ and

$$n = \gamma_w(z - z_w) - \frac{\dot{z}_w^2}{2} \frac{\Delta V}{\sigma} [\gamma_w(z - z_w)]^2 + \mathcal{O}((z - z_w)^4) \quad (74)$$

(the NNLO term vanishes in the expansion of n). To leading order, the coordinate transformation (74) is essentially a Lorentz boost to a coordinate system instantaneously at rest with the wall.

4.2 Small deformations

Let us now consider small deformations of a planar wall. For an infinitely thin wall, we write $z_{w0} = z_{\text{pl}0}(t) + \delta z_0(t, x, y)$, where $z_{\text{pl}0}$ is a solution of the planar-wall EOM, Eq. (69), and δz_0 is a small perturbation. Keeping terms up to linear order in δz_0 in Eq. (60), we obtain the equation

$$\partial_t(\gamma_{\text{pl}0}^3 \partial_t \delta z_0) - \gamma_{\text{pl}0}(\partial_x^2 \delta z_0 + \partial_y^2 \delta z_0) = 0. \quad (75)$$

To go beyond the zero-thickness approximation for both the background solution and the perturbation, we write $z_w = z_{\text{pl}}(t) + \delta z(t, x, y)$, where z_{pl} fulfills the NNLO planar wall EOM, Eq. (71), and we keep terms up to linear order in δz in Eq. (61). We obtain

$$\partial_t(\gamma_{\text{pl}}^3 \partial_t \delta z) - \gamma_{\text{pl}}(\partial_x^2 + \partial_y^2) \delta z = -\frac{l_0^2}{L_0^2} \gamma_{\text{pl}0}(\partial_x^2 + \partial_y^2) \delta z_0. \quad (76)$$

With the convenient change of variables $dt = \gamma_{\text{pl}0} d\tau_0$, $\delta z_0 = \xi_0/\gamma_{\text{pl}0}$, Eq. (75) becomes

$$(\partial_{\tau_0}^2 - \partial_x^2 - \partial_y^2) \xi_0 - L_0^{-2} \xi_0 = 0. \quad (77)$$

This equation was previously derived in Ref. [21] (for the case $\dot{z}_{i0} = 0$) using a covariant gauge. From Eq. (72), we have $\gamma_{\text{pl}0} = \sqrt{1 + (t/L_0 + \gamma_{i0}\dot{z}_{i0})^2}$ and we obtain

$$\tau_0 = L_0 [\text{arcsinh}(t/L_0 + \gamma_{i0}\dot{z}_{i0}) - \text{arcsinh}(\gamma_{i0}\dot{z}_{i0})]. \quad (78)$$

Similarly, with the change of variables $dt = \gamma_{\text{pl}} d\tau$, $\delta z = \xi/\gamma_{\text{pl}}$, Eq. (76) becomes

$$(\partial_{\tau}^2 - \partial_x^2 - \partial_y^2) \xi - L^{-2} \xi = -(l_0/L_0)^2 (\partial_x^2 + \partial_y^2) \xi_0. \quad (79)$$

From Eq. (73), we have $\gamma_{\text{pl}} = \sqrt{1 + (t/L + \gamma_i\dot{z}_i)^2}$ and we obtain

$$\tau = L [\text{arcsinh}(t/L + \gamma_i\dot{z}_i) - \text{arcsinh}(\gamma_i\dot{z}_i)]. \quad (80)$$

The LO equation (77) has solutions of the form $\xi_0 = A_0 e^{i(\mathbf{k}\cdot\mathbf{x}\pm\omega_0\tau)}$, where $\mathbf{x} = (x, y)$, $\mathbf{k} = (k_x, k_y)$, and $\omega_0 = \sqrt{k^2 - L_0^{-2}}$, with $k^2 = k_x^2 + k_y^2$. As noticed in [21], although this solution for ξ_0 grows exponentially with τ_0 for $k^2 < L_0^{-2}$, these modes do not have an exponential growth in the variable t , and, furthermore, the gamma factor in $\delta z_0 = \xi_0/\gamma_{\text{pl}0}$ causes δz_0 to actually decrease with t .⁴ For the other modes, ξ_0 oscillates with frequency ω_0 with respect to τ_0 . With respect to t , these oscillations become increasingly slower, and, besides, δz_0 decreases as $\gamma_{\text{pl}0}^{-1}$. Let us consider for concreteness the initial conditions $\dot{z}_{i0} = 0$ and $\partial_t \delta z_0 = 0$. We have

$$\delta z_0 = A_0 \frac{\cos[\omega_0 L_0 \operatorname{arcsinh}(t/L_0)]}{\sqrt{1 + (t/L_0)^2}} \cos(\mathbf{k} \cdot \mathbf{x}). \quad (81)$$

For the NNLO equation (79), we may propose a solution of the form $A(\tau)e^{i\mathbf{k}\cdot\mathbf{x}}$. The equation for $A(\tau)$ is that of a harmonic oscillator subjected to an external force, which can be solved analytically. However, a simpler approach in this case is to just use the approximation $\xi_0 = \xi$ in the NNLO term. This approximation will be valid as long as both l_0/L_0 and $l_0 k$ are small, since the wall has a local spatial curvature of order k . The solutions are of the form $\xi = A e^{i(\mathbf{k}\cdot\mathbf{x}\pm\omega\tau)}$, with $\omega = \sqrt{(1 - l_0^2/L_0^2)k^2 - L^{-2}}$. For the initial conditions $\dot{z}_i = 0$ and $\partial_t \delta z = 0$, we have

$$\delta z = A \frac{\cos[\omega L \operatorname{arcsinh}(t/L)]}{\sqrt{1 + (t/L)^2}} \cos(\mathbf{k} \cdot \mathbf{x}). \quad (82)$$

According to Eqs. (62)-(66), the variations of the surface will induce variations of σ and l which depend on the quantity $\partial_n K_0$. Using Eqs. (69) and (75) in Eq. (67), we have

$$\partial_n K_0|_0 = L_0^{-2} + 2L_0^{-1}\gamma_{\text{pl}0}(\partial_x^2 + \partial_y^2)\delta z_0. \quad (83)$$

For the solution (81), we have

$$\partial_n K_0|_0 = L_0^{-2} - 2L_0^{-1}A_0 k^2 \cos[\omega_0 L_0 \operatorname{arcsinh}(t/L_0)] \cos(\mathbf{k} \cdot \mathbf{x}). \quad (84)$$

The constant term in Eq. (84) is already present for a planar wall and is due to the global acceleration. Since we have $\delta l \propto \partial_n K_0|_0$, we see how the spatial undulations of the surface are transmitted to the wall width. According to Eq. (84), these variations do not decrease with time in the wall frame. However, for an observer at rest at $z = 0$, they do decrease due to the Lorentz contraction.

4.3 Spherical wall

In spherical coordinates $x^a = \xi^a = t, \theta, \varphi$ and $x^3 = r$, we have a diagonal metric given by $g_{00} = 1, g_{rr} = -1, g_{\theta\theta} = -r^2, g_{\varphi\varphi} = -r^2 \sin^2 \theta$. In the Monge representation, the position of the wall is described by $r = r_w(t, \theta, \varphi)$. We will consider for simplicity the case of a spherical wall, $r = r_w(t)$. Thus, Eq. (1) gives $N_t = \gamma_w \dot{r}_w, N_r = -\gamma_w$, with $\gamma_w = 1/\sqrt{1 - \dot{r}_w^2}$, and the other components of the normal vector vanish. The only

⁴Taking $\dot{z}_{i0} = 0$ for simplicity, we have $e^{\pm i\omega_0\tau_0} = (t/L_0 + \gamma_{\text{pl}0})^{\pm\sqrt{1-(kL_0)^2}}$, with $\gamma_{\text{pl}0} = \sqrt{1 + (t/L_0)^2}$. Therefore, we have $e^{\pm i\omega_0\tau_0}/\gamma_{\text{pl}0} \sim t^{\pm\sqrt{1-(kL_0)^2}-1}$ for $t \rightarrow \infty$.

non-zero Christoffel symbols that appear in Eq. (11) are $\Gamma_{r\theta}^\theta = r^{-1}$ and $\Gamma_{r\varphi}^\varphi = r^{-1}$, and Eqs. (55) and (59) give

$$\gamma_{w0}^3 \ddot{r}_{w0} + 2 \frac{\gamma_{w0}}{r_{w0}} = \frac{\Delta V}{\sigma_0}, \quad (85)$$

$$\gamma_w^3 \ddot{r}_w + \frac{2\gamma_w}{r_w} = \frac{\Delta V}{\tilde{\sigma}} + l_0^2 \frac{\Delta V}{\sigma_0} \left[(\gamma_{w0}^3 \ddot{r}_{w0})^2 + 2 \frac{\gamma_{w0}^2}{r_{w0}^2} \right] - l_0^2 \left[(\gamma_{w0}^3 \ddot{r}_{w0})^3 + 2 \frac{\gamma_{w0}^3}{r_{w0}^3} \right], \quad (86)$$

while the NLO equation takes the same form as the LO equation, with the replacement $\sigma_0 \rightarrow \sigma_0 + \sigma_1$. Using (85) in (86), we obtain

$$\gamma_w^3 \ddot{r}_w + \frac{2\gamma_w}{r_w} = \frac{\Delta V}{\tilde{\sigma}} + 2l_0^2 \frac{\gamma_{w0}}{r_{w0}} \left[\left(\frac{\Delta V}{\sigma_0} \right)^2 - 3 \frac{\Delta V}{\sigma_0} \frac{\gamma_{w0}}{r_{w0}} + 3 \left(\frac{\gamma_{w0}}{r_{w0}} \right)^2 \right]. \quad (87)$$

The case $\Delta V = 0$ (domain wall), has already been considered in Ref. [10]. At leading order, the wall collapses due to the surface tension. The NNLO correction, which is proportional to $r_{w0}^{-3} \gamma_{w0}^3$, slows down the collapse and eventually prevents it. However, for small enough r_w , the perturbative expansion will break down.

For $\Delta V \neq 0$, the first term on the right-hand side of Eq. (87) is like at leading order, with the replacement $\sigma_0 \rightarrow \tilde{\sigma}$. It is not difficult to see that the term proportional to l_0^2 is always positive. The case $\Delta V < 0$ corresponds to a false-vacuum bubble and, for a vacuum phase transition, has been studied mainly in curved spacetime (see, e.g., [35–39]). In flat space, such a bubble will collapse. This case may apply to a thermal phase transition with subcritical bubbles [40–42] or to the evolution of false-vacuum domains after bubble percolation [43, 44]. Like in the domain wall case, the correction proportional to l_0^2 in Eq. (87) opposes the collapse of the bubble. For $\Delta V > 0$, the bubble can expand or collapse, depending on whether the pressure difference or the surface tension dominates. This is easily seen in the leading order equation (85), where we have a critical radius, $r_{c0} = 2\sigma_0/\Delta V$, for which a bubble with $\dot{r}_{w0} = 0$ is in unstable equilibrium. This case may be relevant for the dynamics of phase mixing in phase transitions with subcritical bubbles. The NNLO corrections shift the critical radius and slow down the bubble collapse. We shall focus here on the case of an expanding bubble and address the other possibilities elsewhere.

We define the parameter $R_0 = 3L_0 = 3\sigma_0/\Delta V$, which is the relevant length scale associated to the curvature in the spherical case⁵. For convenience of notation, we also define the parameter $\tilde{R} = 3\tilde{\sigma}/\Delta V$. The latter is not directly related to the curvature, since the term proportional to l_0^2 in Eq. (87) never vanishes [cf. Eqs. (57)–(58)].

To solve Eq. (85), we multiply it by $r_{w0}^2 \dot{r}_{w0}$ and integrate. With the initial conditions $r_{w0} = r_{i0}$, $\gamma_{w0} = \gamma_{i0}$ at $t = 0$, we obtain

$$\gamma_{w0} r_{w0}^2 - \gamma_{i0} r_{i0}^2 = R_0^{-1} (r_{w0}^3 - r_{i0}^3). \quad (88)$$

Solving for \dot{r}_{w0} and integrating again, we obtain the implicit solution

$$\int_{r_{i0}}^{r_{w0}} \frac{dr}{\sqrt{1 - (r/R_0 - \beta_0 r_{i0}^2/r^2)^{-2}}} = t, \quad (89)$$

⁵Like in the planar case, we have a constant mean curvature $K_0|_0 = \Delta V/\sigma_0 = L_0^{-1}$. However, in the spherical case we have three non-vanishing eigenvalues k_i (associated to the space curvature and the acceleration). If the hypersurface is O(3,1) invariant, these eigenvalues are equal and the trace is $K_0 = 3k_i$. This gives $k_i = K_0/3$ and $R_0 = 3L_0$. In Sec. 6 we discuss this symmetric case.

where $\beta_0 = r_{i0}/R_0 - \gamma_{i0}$. Similarly, we multiply Eq. (87) by $r_w^2 \dot{r}_w$ (taking into account that, in the highest-order term, we have $r_w \simeq r_{w0}$) and integrate. We obtain

$$\gamma_w r_w^2 - \gamma_i r_i^2 = \tilde{R}^{-1} (r_w^3 - r_i^3) + l_0^2 [2R_0^3 (r_{w0}^3 - r_{i0}^3) + \beta_0^3 r_{i0}^6 (r_{w0}^{-6} - r_{i0}^{-6})], \quad (90)$$

where $r = r_i$, $\gamma = \gamma_i$ are the initial conditions at $t = 0$. Solving for \dot{r}_w and integrating again (and neglecting orders higher than l_0^2), we obtain

$$\int_{r_i}^{r_w} \frac{dr}{\sqrt{1 - (r/\tilde{R} - \beta r_i^2/r^2)^{-2}}} = t + \frac{l_0^2}{R_0^2} \int_{r_{i0}}^{r_{w0}} \frac{\frac{2r}{R_0} - \left(\frac{2r_{i0}^3}{R_0^3} + \beta_0^3\right) \frac{R_0^2}{r^2} + \frac{R_0^2 \beta_0^3 r_{i0}^6}{r^8}}{[(r/R_0 - \beta_0 r_{i0}^2/r^2)^2 - 1]^{3/2}} dr, \quad (91)$$

where $\beta = r_i/\tilde{R} - \gamma_i$.

At leading order, the critical radius between expansion and collapse is $r_{c0} = 2L_0$. Another special situation occurs when the initial conditions fulfill $r_{i0} = \gamma_{i0}R_0$, so that we have $\beta_0 = 0$ (this condition requires $r_{i0} \geq 3L_0 > r_{c0}$). In this case, Eq. (88) becomes $\gamma_{w0} = r_{w0}/R_0$, i.e., the initial relation holds at all time, and the solution (89) takes the same form as in the 1+1-dimensional case (72), $r_{w0}^2 = R_0^2 + (t + R_0\gamma_{i0}\dot{r}_{i0})^2$. With the additional initial condition $\dot{r}_{i0} = 0$, we obtain the well-known O(3,1)-invariant solution $r_{w0}^2 = R_0^2 + t^2$. The values $\dot{r}_{i0} = 0$, $r_{i0} = R_0$ are well-motivated initial conditions for the nucleated bubble since they are obtained in the thin-wall approximation for the instanton [32]. The NNLO equation, Eq. (91), becomes simpler⁶ for $\dot{r}_i = 0$ and $r_i = \tilde{R}$. However, there is no actual motivation for this initial condition, since the resulting solution is not O(3,1) invariant. Neither does the value $\tilde{R} = 3\tilde{\sigma}/\Delta V$ give the best estimate for the nucleation radius, which we address in Sec. 6.

Using Eqs. (85) and (88) in Eq. (11), we obtain

$$\partial_n K_0|_{n=0} = \left(\frac{1}{L_0} - 2\frac{\gamma_{w0}}{r_{w0}}\right)^2 + 2\frac{\gamma_{w0}^2}{r_{w0}^2} = 3R_0^{-2} + 6\beta_0^2 r_{i0}^4 r_{w0}^{-6}. \quad (92)$$

On the other hand, all the Christoffel symbols that appear in Eq. (7) vanish for the spherical case. Using the above results, we obtain

$$n = \gamma_w(r - r_w) - \frac{\dot{r}_w^2}{2} \left(\frac{3}{\tilde{R}} - \frac{2\gamma_w}{r_w}\right) [\gamma_w(r - r_w)]^2 - \frac{\dot{r}_w^4 \gamma_w}{r_w} \left(\frac{1}{R_0} - \frac{\gamma_w}{r_w}\right) [\gamma_w(r - r_w)]^3. \quad (93)$$

5 Specific examples

To illustrate our results, we will now consider the simple potential

$$V(\phi) = \frac{1}{2}m^2\phi^2 - \frac{e}{3}\phi^3 + \frac{\lambda}{4}\phi^4, \quad (94)$$

where we have $\phi_+ = 0$, $\phi_- = (e/2\lambda)(1 + \sqrt{1 - 4\lambda m^2/e^2})$, and the maximum between the two minima is at $\phi_b = e/\lambda - \phi_-$. For $\lambda m^2/e^2 < 2/9$, we have $V_+ = 0$, $V_- = -\frac{1}{4}\phi_-^2 (\frac{e}{3}\phi_- - m^2) < 0$, and $V_b \equiv V(\phi_b) = \frac{1}{4}\phi_b^2 (m^2 - \frac{e}{3}\phi_b)$. We will construct the degenerate potential

⁶Neglecting terms of order higher than l_0^2 , we obtain $r_w = \sqrt{\tilde{R}^2 + t^2} - \frac{2l_0^2}{R_0^2} \left(\frac{R_0^3}{r_{w0}^3} + \frac{R_0^2}{r_{w0}^2} - 2\frac{R_0}{r_{w0}}\right)$.

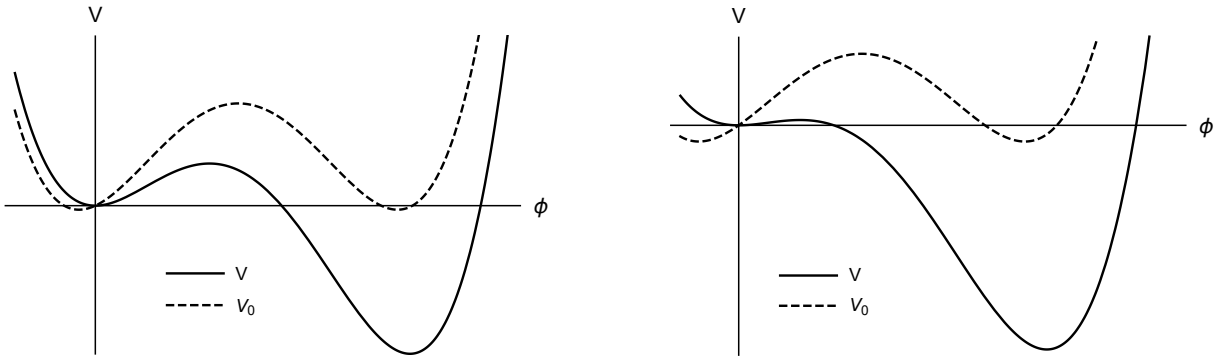


Figure 1: The shape of the potentials (94) and (95). Left panel: $\lambda = 0.5$, $e/m = 1.6$, and $\Delta V/V_b \simeq 3.5$. Right panel: $\lambda = 0.5$, $e/m = 1.9$, and $\Delta V/V_b \simeq 42$.

V_0 with a linear term $\tilde{V}(\phi) = c\phi$. The conditions (17)-(18) give $c = e(9\lambda m^2 - 2e^2)/27\lambda^2$, and we have

$$V_0(\phi) - V_{0\pm} = \frac{\lambda}{4} (\phi - a_+)^2 (\phi - a_-)^2, \quad (95)$$

with $a_{\pm} = \frac{e}{3\lambda} (1 \mp \sqrt{1 - 27c\lambda^2/e^3})$. As discussed in Sec. 2, the thin-wall approximation is expected to work well when $\Delta V/V_b \ll 1$. In our previous work [30], we showed that the LO and NLO approximations work quite well even when we have $\Delta V/V_b \sim 1$. Here, we will consider two parameter sets which give $\Delta V/V_b \simeq 3.5$ and $\Delta V/V_b \simeq 42$ (see Fig. 1).

5.1 Wall profile and EOM parameters

The functions of n obtained in Sec. 3 can be written as functions of ϕ_0 by means of Eq. (25), and the integrals with respect to n can be written as integrals with respect to the field, like in Eq. (26). This simplifies the calculations by avoiding the explicit use of the solution $\phi_0(n)$. We write down the expressions in App. B. For this specific potential, we obtain analytic results for most of the quantities, which we also write down in App. B. In particular, we have

$$\phi_0(n) = \phi_* - a \tanh(\sqrt{\lambda/2} a n), \quad (96)$$

where $\phi_* = (a_+ + a_-)/2$ and $a = (a_- - a_+)/2$. The LO wall width is given by

$$l_0 = \sqrt{(\pi^2/6 - 1)} (\sqrt{\lambda} a)^{-1}. \quad (97)$$

For the potential on the left panel of Fig. 1 we have $l_0/L_0 \simeq 0.3$, while for that on the right panel, we have $l_0/L_0 \simeq 0.54$.

With the linear modification $\tilde{V} = c\phi$, we obtain

$$\phi_1 = -c/(2a^2\lambda). \quad (98)$$

Since ϕ_1 is a constant, according to Eq. (35), the NLO quantities $I_1^{(k)}$, $\bar{I}_1^{(k)}$ vanish. In particular, we have $\sigma_1 = \mu_1 = 0$, so, to next-to-leading order, we still have $l = l_0$. As discussed in [30], these characteristics of the NLO corrections are a consequence of the simplicity of the quartic potential and the linear modification, and do not occur for other potentials or modifications. Nevertheless, the overall quantitative results are similar. For

example, although the correction σ_1 vanishes in this case, the approximation σ_0 is already as good as $\sigma_0 + \sigma_1$ for other potentials or modifications.

For the NNLO quantities, we also obtain analytic expressions (which can be found in App. B), except for the parameter α . The constants c_{2a} and c_{2b} vanish in this case, so we have

$$\phi_2 = \phi_h(\phi_0) [C_{2a}(\phi_0) + C_{2b}(\phi_0)\partial_n K_0|_0]. \quad (99)$$

Using the results for σ_i and μ_i in Eqs. (65)-(66), we obtain

$$\frac{l}{l_0} = 1 + \frac{3c^2}{8\lambda^2 a^6} + \frac{1}{2} \left(\frac{\pi^2}{6} - 1 + \frac{0.346305}{\pi^2/6 - 1} \right) \frac{\partial_n K_0|_0}{\lambda a^2}. \quad (100)$$

The constant correction proportional to c^2 comes from the term \tilde{V} which breaks the degeneracy of the potential, and is due to the wall acceleration.

5.2 Evolution of a thick spherical bubble

For a spherical bubble, the LO radius r_{w0} is given by Eq. (89) and depends on the parameter $R_0 = 3L_0 = 3\sigma_0/\Delta V$ and the initial conditions r_{i0}, γ_{i0} . The NLO radius has the same form, with the parameter σ_0 replaced by $\sigma_0 + \sigma_1$. Moreover, for the specific potentials V and V_0 given by Eqs. (94)-(95), we have $\sigma_1 = 0$, so, if we take the same initial conditions, we have the same solution r_{w0} . The NNLO bubble radius is given by Eq. (91) and depends on the parameter \tilde{R} and the initial conditions r_i, γ_i , as well as on the LO solution. On the other hand, the total NNLO field profile is given by Eq. (50), where $\partial_n K_0|_0$ is given by Eq. (92) and the ϕ_i are given by Eqs. (96), (98), and (99), with the variable n given by Eq. (93).

In order to compare these results with a numerical solution of the field equation, we will solve Eq. (2) for the O(3,1)-symmetric case, which simplifies the numerical computation. Notice that our perturbative treatment gives an equation of motion for the wall surface but does not provide initial conditions, i.e., it gives the wall evolution from an initial surface. In the present case, we will set $r_{i0} = r_i = \bar{r}$, where we will calculate the initial radius \bar{r} from the numerical profile. For the particular case of the O(3,1)-symmetric solution we could, alternatively, set $r_{i0} = R_0$, which is the value one obtains by considering the nucleation process in the usual thin-wall approximation [32]. However, to be consistent with our NNLO EOM, we should use a better estimation for the initial value r_i . We consider this alternative in Sec. 6, but here we will just obtain the initial conditions from the numerical solution, so that we can verify how well our perturbative expansion approximates the subsequent evolution of the wall.

Assuming a solution of Eq. (2) of the form $\phi(x^\mu) = \bar{\phi}(\rho)$, with $\rho^2 = \mathbf{x}^2 - t^2$, we obtain the well-known equation [32]

$$\frac{d^2 \bar{\phi}}{d\rho^2} + \frac{3}{\rho} \frac{d\bar{\phi}}{d\rho} = V'(\bar{\phi}) \quad (101)$$

with the boundary conditions

$$\frac{d\bar{\phi}}{d\rho}(0) = 0, \quad \lim_{\rho \rightarrow \infty} \bar{\phi}(\rho) = \phi_+. \quad (102)$$

This equation is usually solved numerically using the overshoot-undershoot method. Actually, this method gives only the part of the profile for $r \geq t$ (real ρ). To numerically

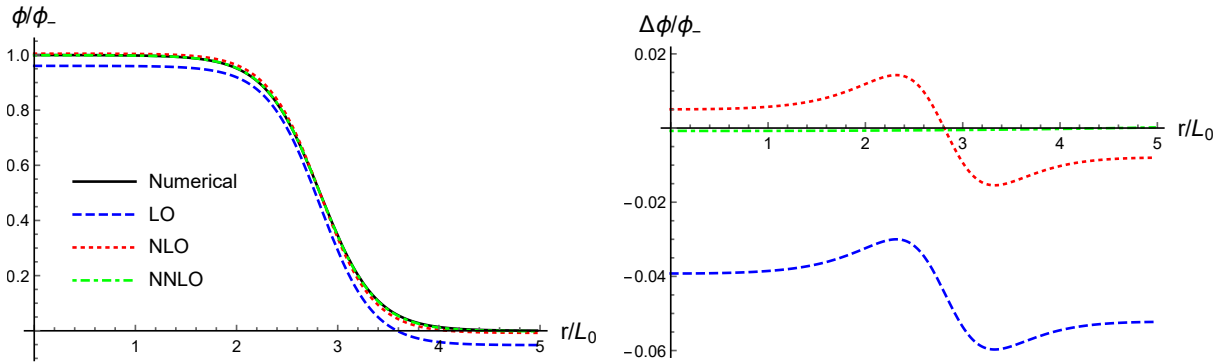


Figure 2: Bubble profile at $t = 0$ for the potential shape shown in the left panel of Fig. 1 ($\Delta V/V_b \simeq 3.5$, $l_0/L_0 \simeq 0.3$). Left: The numerical solution and the analytical approximations. Right: The difference of each approximation with the numerical solution.

obtain the profile for $r < t$, Eq. (101) can be analytically continued, which essentially consists in changing the sign of the potential. The boundary conditions for this part of the profile are just the matching conditions with the usual solution at $\rho = 0$ [30, 45]. We define the wall position \bar{r}_w for the numerical solution as the average of r weighted with the function $(\partial_r \phi)^2$,

$$\bar{r}_w = \frac{\int_t^\infty (\partial_r \phi)^2 r dr}{\int_t^\infty (\partial_r \phi)^2 dr}. \quad (103)$$

The limit of integration $r = t$ corresponds to $\rho = 0$, which can be regarded as the boundary between the wall and the bubble interior.

We remark that our perturbative solution for the profile, Eq. (50), does not take the simple form $\phi(\rho)$ but depends on x^μ through the quantities n and $\partial_n K_0|_0$. To obtain such a Lorentz-invariant solution in the thin wall approximation, we must consider the field ϕ as a function of ρ from the beginning. We discuss this approach in Sec. 6. Of course, with the appropriate initial conditions, our general approach will give a good approximation for this particular case as well, only the symmetry is not explicit in the perturbative expansion. We use the values $\gamma_{i0} = \gamma_i = 1$, $r_{i0} = r_i = \bar{r}_w(0)$ as initial conditions for our LO and NNLO solutions, Eqs. (89) and (91).

In Fig. 2, we consider the case $\Delta V/V_b \simeq 3.5$. The field profile is shown at $t = 0$, where we have $\rho = r$ and $n = r - r_i$. We see that the NLO approximation is not bad, but the NNLO approximation is much better. For more clarity, the right panel shows the difference between the numerical solution and the approximations. At later times, the main variation of these profiles will be the change of their position and the Lorentz contraction of the wall width. The different approximations for r_w are shown in the left panel of Fig. 3. We see that the NNLO approximation is much better than the LO one (for this potential, the NLO approximation coincides with the latter since we have $\sigma_1 = 0$).

In the right panel of Fig. 3 and in Fig. 4, we consider the case $\Delta V/V_b \simeq 42$. We see that the NNLO approximation for r_w works quite well. The maximum relative deviation from the numerical value \bar{r}_w is about 3% (at $t \simeq 3.8L_0$). In contrast, the LO (and NLO) approximation quickly departs from the correct value. Nevertheless, at higher t , all the curves in Fig. 3 become parallel, so the relative differences decrease with time. It is interesting to note that, if we use instead the initial conditions r_{i0}, r_i estimated with the thin-wall approximation at each order, the evolution of the approximations is the opposite,

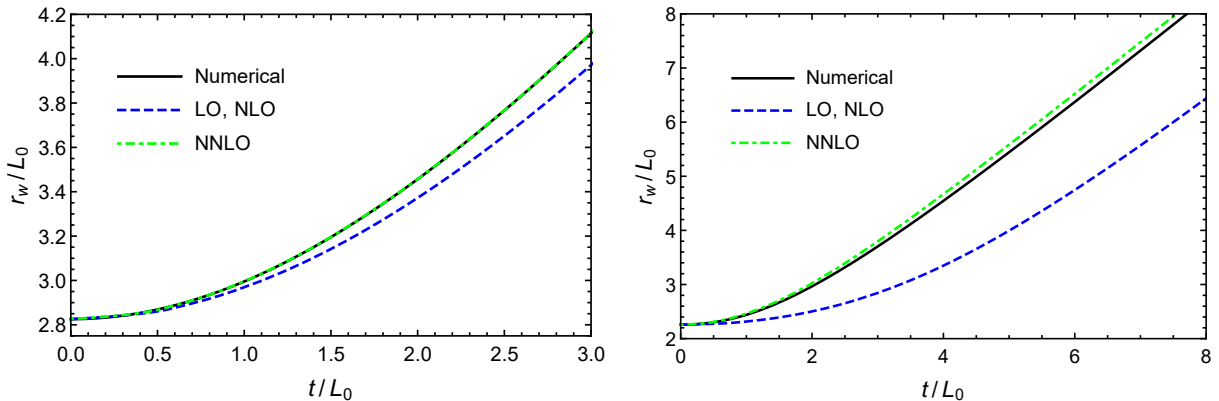


Figure 3: The mean bubble radius for the numerical solution and the thin-wall approximations. The left and right panels correspond to the potential shapes shown in the left and right panels of Fig. 1, respectively.

i.e., the initial values are different from the numerical value, but the curves approach each other at later times (see Sec. 6).

In Fig. 4 we consider the profile at several times. As shown by the black curve in the first plot, the field does not initially take the value $\phi = \phi_-$ inside the nucleated bubble. In contrast, the thin-wall approximation does approach this value (with increasing precision at higher order), and thus fails to reproduce the initial moments of the bubble profile (the fact that the LO curve approaches the value ϕ_- is just a numerical coincidence). At later times, the field inside the bubble is in the potential minimum, and we see that the NNLO curve gives a much better approximation than the LO and NLO curves. Notice, however, that the main error in these curves is due to the wall position rather than to the shape of the profile.

5.3 Perturbations on a planar wall

Let us now consider small sinusoidal perturbations from a planar wall, for the concrete case of the potential with $\Delta V/V_b \simeq 3.5$, for which we have $l_0/L_0 \simeq 0.3$. The unperturbed solution for the wall position is given by Eq. (72) at leading order in the wall thickness and by Eq. (73) at next-to-next-to-leading order. We set the initial conditions $z_i = z_{i0} = L_0$, $\dot{z}_i = \dot{z}_{i0} = 0$. These background solutions are shown in Fig. 5. We see that the NNLO correction to the dynamics is smaller than for the spherical wall (cf. left panel of Fig. 3).

For the perturbations, we shall also consider the same initial conditions at each order, namely, $\delta z = \delta z_0$, with $\delta \dot{z} = \delta \dot{z}_0 = 0$. The LO approximation δz_0 is given by Eq. (81) and the NNLO approximation δz is given by Eq. (82). In Fig. 6, we show the evolution of the amplitude of the perturbations for a few values of the wavenumber k . The NNLO correction is quite larger than in the background solution. This is because the curvature of the hypersurface is no longer given by the acceleration alone (which would give $K = L_0^{-1}$), but the undulations of the surface introduce a curvature of order k^{-1} . Therefore, the expansion in the wall width is an expansion in powers of $l_0 k$ as well as an expansion in l_0/L_0 . For the modes considered in Fig. 6, we have $l_0 k \simeq 0.15, 0.3, 0.6, 0.9$ and 1.2 .

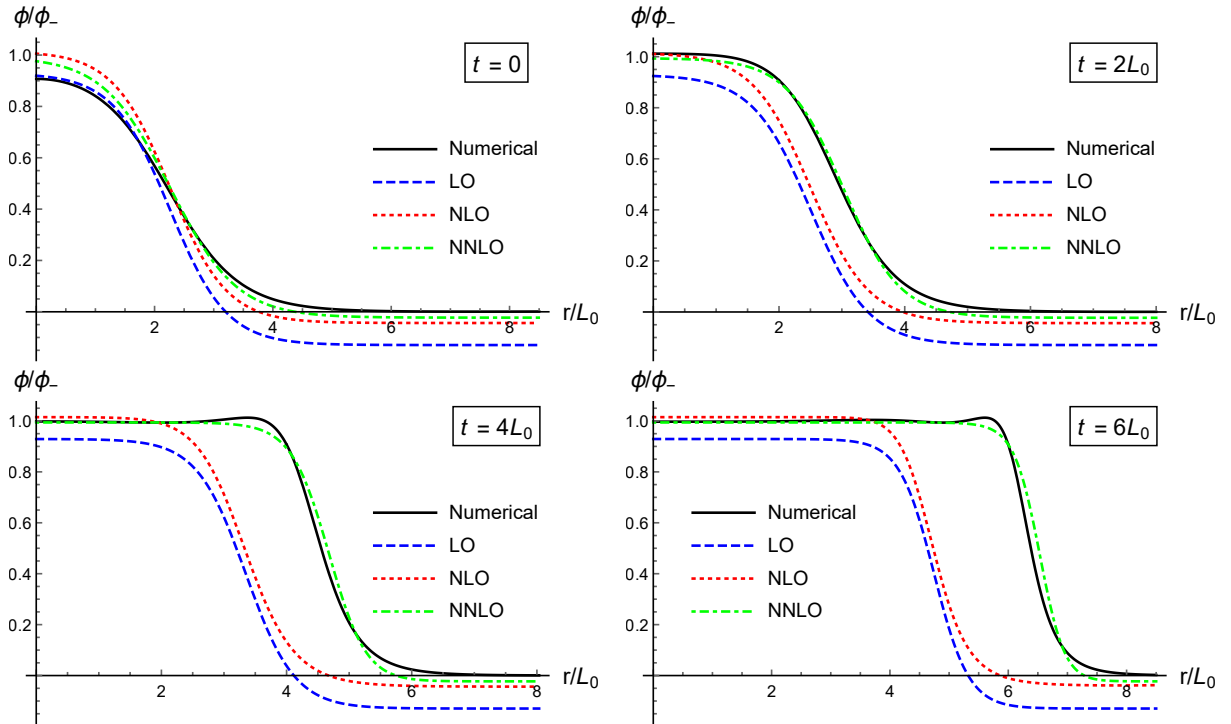


Figure 4: The numerical profile and the approximations for the potential shape shown in the right panel of Fig. 1 ($\Delta V/V_b \simeq 42$, $l_0/L_0 \simeq 0.54$).

Using the result (84) in Eq. (100), we obtain the variations of l ,

$$\frac{l}{l_0} = 1 + \frac{3c^2}{8\lambda^2 a^6} + \frac{0.590948}{\lambda a^2 L_0^2} [1 - 2L_0 A_0 k^2 \cos[\omega_0 L_0 \operatorname{arcsinh}(t/L_0)] \cos(\mathbf{k} \cdot \mathbf{x})]. \quad (104)$$

Besides the constant corrections, which are due to the global acceleration, there are corrections due to the varying curvature of the hypersurface. As a consequence, l oscillates around a fixed value \bar{l} . Fig. 7 shows the variation of l along the wall surface at $t = 0$ and its time variation at a given point (the value \bar{l} is indicated by a dashed line). We see that, the larger the curvature, the stronger the effect. This is to be expected since the variations of the wall width are a consequence of the surface bending.

6 The O(3,1)-invariant bubble

The process of bubble nucleation is described by the bounce instanton [32]. The most probable configuration of the bubble at the moment of its materialization corresponds to the bounce of minimum Euclidean action. The latter is O(4) invariant, and the initial evolution of the bubble, which is the analytic continuation of the bounce, is O(3,1) invariant. Hence, the field is of the form $\phi(x^\mu) = \bar{\phi}(\rho)$, with $\rho = \sqrt{r^2 - t^2}$. In Ref. [32], Coleman considered the leading-order thin-wall approximation for the instanton and applied it to $\bar{\phi}(\rho)$. Here, we shall consider higher orders in the wall width. While in Sec. 3 we obtained a wall EOM which required initial conditions, imposing a symmetric solution will determine the initial bubble radius and wall velocity.

In Sec. 3, we used normal Gaussian coordinates because the field depends only on the variable n at the lowest orders in the wall width. However, if we assume that the exact

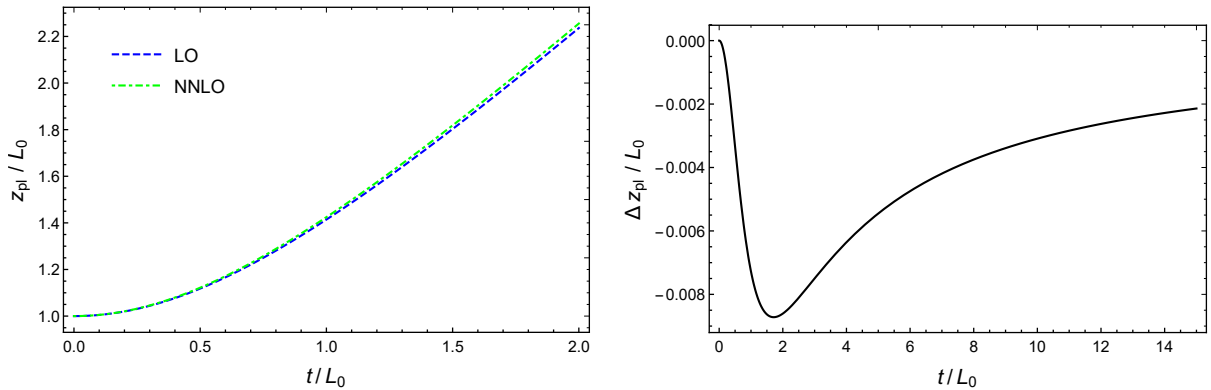


Figure 5: LO and NNLO solutions for the position z_{pl} of a planar wall (left) and their difference Δz_{pl} (right).

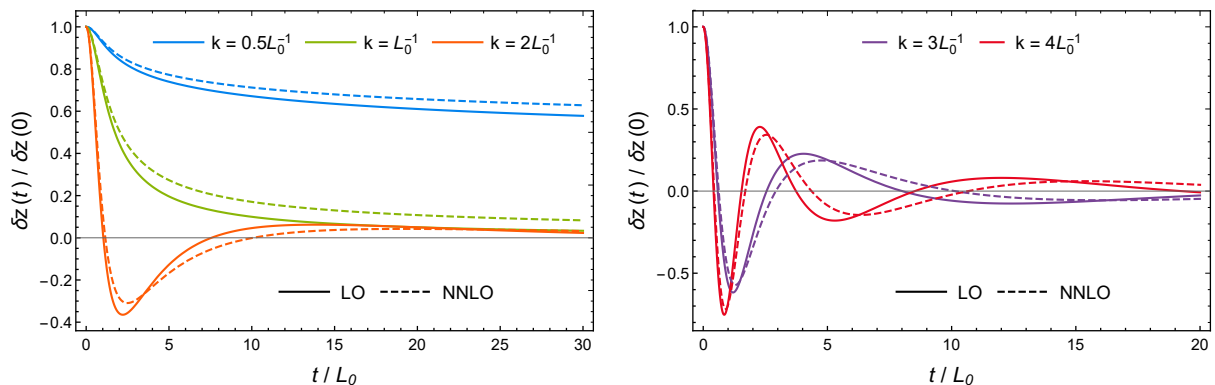


Figure 6: The amplitude of sinusoidal deformations.

solution depends only on ρ , the dependence on a single variable must be valid at every order in the wall width. In particular, the exact field equation in terms of ρ , which is given by Eq. (101), takes the same form of the approximation (12), with $K = -3/\rho$. We need to adapt our method to use the variable ρ instead of n . This will give an explicitly Lorentz-invariant solution at each order.

With the assumption that ϕ is a function of ρ only, the treatment is much simpler than in Sec. 3. A fixed point in the field profile corresponds to a fixed value of ρ . Therefore, if we define the wall hypersurface by $\phi(x^\mu) = \phi_w$, where ϕ_w is some reference value between ϕ_+ and ϕ_- , we have the condition $\rho(x^\mu) = \rho_w$, where $\bar{\phi}(\rho_w) = \phi_w$. This condition determines the form of the solution for the bubble radius, namely, $r = r_w(t)$, with

$$r_w^2 = \rho_w^2 + t^2. \quad (105)$$

Thus, we do not need to solve an equation of motion but only calculate the value of the constant ρ_w , which also gives the initial bubble radius.

We may define the reference value ρ_w as the weighted average

$$\rho_w = \sigma^{-1} \int_0^\infty \bar{\phi}'(\rho)^2 \rho d\rho, \quad (106)$$

where $\sigma = \int_0^\infty \bar{\phi}'(\rho)^2 d\rho$. As usual, we will make the approximation that the field takes the value $\phi = \phi_-$ inside the bubble. This value will be reached asymptotically at $\rho = -\infty$

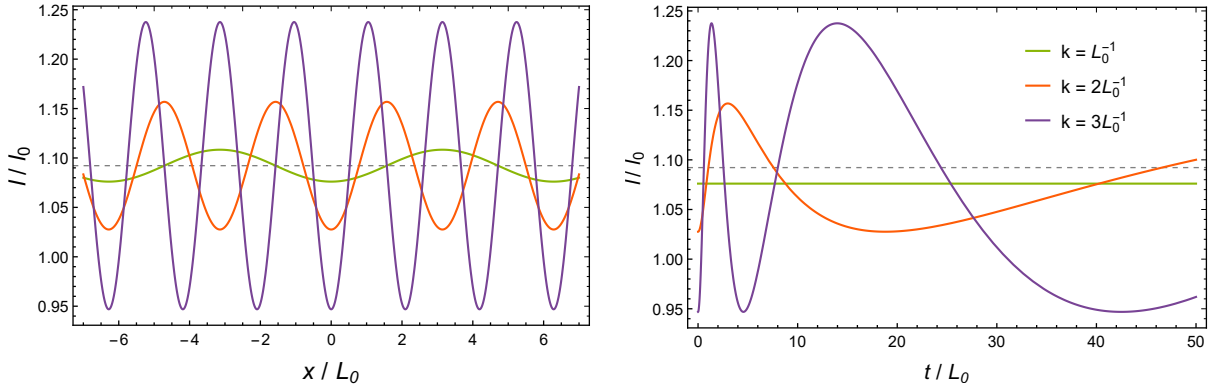


Figure 7: Variations of the wall width l when the surface has sinusoidal deformations of amplitude $A_0 = 0.1L_0$ ($A_0/l_0 \simeq 0.34$).

instead of $\rho = 0$. Therefore, we must replace the limit of integration $\rho = 0$ with $\rho = -\infty$ in the expressions above. For a discussion of these approximations, see [30]. The role of the variable n in Sec. 3 is played here by $\eta = \rho - \rho_w$. Indeed, in terms of η , Eq. (106) becomes $\int_{-\infty}^{+\infty} \bar{\phi}'^2 \eta d\eta = 0$, which is similar to the condition (21).

Multiplying Eq. (101) by $d\bar{\phi}/d\rho$ and integrating, we obtain a first integral which, in terms of η , takes the form

$$\frac{1}{2} \left(\frac{d\bar{\phi}}{d\eta} \right)^2 + \int_{\infty}^{\eta} \frac{3}{\rho_w + \tilde{\eta}} \left(\frac{d\bar{\phi}}{d\tilde{\eta}} \right)^2 d\tilde{\eta} = V(\bar{\phi}) - V_+. \quad (107)$$

Evaluating Eq. (107) at $\eta = -\infty$, we obtain the equation

$$\int_{-\infty}^{+\infty} \frac{3}{\rho_w + \eta} \left(\frac{d\bar{\phi}}{d\eta} \right)^2 d\eta = \Delta V. \quad (108)$$

The last two equations replace Eqs. (19) and (20). To lowest order in the wall width, we neglect the term proportional to $K = -3/\rho$ in Eq. (107) and replace V with the degenerate potential V_0 . Thus, Eq. (107) takes the form of Eq. (24), and we obtain the solution $\bar{\phi}(\rho) = \phi_0(\eta)$, with ϕ_0 given by Eq. (25). Like in Sec. 3, to calculate $\bar{\phi}$ to higher order, we write

$$\bar{\phi}(\rho) = \phi_0(\eta) + \phi_1(\eta) + \phi_2(\eta) + \dots. \quad (109)$$

We also expand of $3/\rho$ as a series in η and separate ρ_w into terms of different orders,

$$\frac{3}{\rho_w + \eta} = \frac{3}{\rho_w} - \frac{3}{\rho_w^2} \eta + \dots, \quad \rho_w = \rho_0 + \rho_1 + \dots. \quad (110)$$

Inserting these expansions in Eq. (107), we obtain Eqs. (36) for $\phi_i(\eta)$, with the quantities f_i given by Eqs. (37)-(39), but with

$$K_0|_0 = -\frac{3}{\rho_0}, \quad K_1|_0 = \frac{3\rho_1}{\rho_0^2}, \quad K_2|_0 = \frac{3\rho_2}{\rho_0^2} - \frac{3\rho_1^2}{\rho_0^3}, \quad (111)$$

$$\partial_n K_0|_0 = \frac{3}{\rho_0^2}, \quad \partial_n K_1|_0 = -\frac{6\rho_1}{\rho_0^3}, \quad \partial_n^2 K_0|_0 = -\frac{6}{\rho_0^3}. \quad (112)$$

The functions $\phi_i(\eta)$ are thus given by the solution (43), but there is no dependence on ξ^a . On the other hand, evaluating Eq. (36) at $\eta = -\infty$ gives $f_i = 0$, which is equivalent to considering the perturbative expansion of Eq. (108). We obtain

$$\frac{3\sigma_0}{\rho_0} = \Delta V_1, \quad \frac{3\sigma_1}{\rho_0} - \frac{3\rho_1}{\rho_0^2}\sigma_0 = \Delta V_2, \quad \frac{3\sigma_2}{\rho_0} - \frac{3\rho_1\sigma_1}{\rho_0^2} - \frac{3\rho_2\sigma_0}{\rho_0^2} + \frac{3\rho_1^2\sigma_0}{\rho_0^3} + \frac{3\mu_0}{\rho_0^3} = \Delta V_3, \quad (113)$$

with ΔV_i defined below Eqs. (30)-(31) and σ_i, μ_i defined below Eq. (35). The first of Eqs. (113) gives the radius ρ_w to leading order, $\rho_0 = 3\sigma_0/\Delta V_1$. Hence, to this order, we can write $\rho_w = 3\sigma_0/\Delta V = R_0$, which is the well known result. Adding the first two equations in (113), we obtain

$$\rho_0 + \rho_1 \simeq \frac{3(\sigma_0 + \sigma_1)}{\Delta V_1 + \Delta V_2}, \quad (114)$$

which again gives $\rho_w = 3\sigma/\Delta V$. Adding the three equations, we obtain

$$\rho_w \simeq \frac{3(\sigma_0 + \sigma_1 + \sigma_2)}{\Delta V_1 + \Delta V_2 + \Delta V_3} + \frac{\Delta V_1 \mu_0}{3\sigma_0 \sigma_0} \simeq \frac{3\sigma}{\Delta V} + \frac{l_0^2}{\rho_0}. \quad (115)$$

The quantities σ_i and μ_i have the same expressions as in Sec. 3. In particular, we have $\sigma_2 = \tilde{\sigma}_2 - \mu_0 \partial_n K_0$, where, in this case, we have $\partial_n K_0|_0 = 3/\rho_0^2$. Hence, we have

$$\rho_w = \frac{3\tilde{\sigma}}{\Delta V} - 2\frac{l_0^2}{\rho_0} \equiv R. \quad (116)$$

Finally, the field profile is given by Eq. (50), where the functions ϕ_i are the same as in Sec. 3 with n replaced by η , and $\partial_n K_0|_0 = 3/\rho_0^2$.

As already discussed, the O(3,1) solution is the analytic continuation of the O(4) bounce instanton. We could have equivalently considered the Euclidean case by using the imaginary time version of ρ , namely, $\rho = \sqrt{\tau^2 + r^2}$. Thus, ρ_w gives the radius of the nucleated bubble. For the potential considered in Sec. 5, Eq. (106) gives a numerical value $\rho_w \simeq 2.83L_0$ for the case with $\Delta V/V_b \simeq 3.5$ and $\rho_w \simeq 2.26L_0$ for the case with $\Delta V/V_b \simeq 42$. The leading order approximation $\rho_w = R_0 = 3L_0$ has an error of 6% in the first case and of 33% in the second case, while the NNLO approximation $\rho_w = R$ has an error of 0.5% in the first case and of 8% in the second case⁷. In Fig. 8 we plot the bubble radius $r_w = \sqrt{\rho_w^2 + t^2}$ for the different approximations for ρ_w . Notice that the radius $\bar{r}_w(t)$, defined in Eq. (103) as a spatial average, will not coincide exactly with this Lorentz-invariant form. It corresponds to a different definition of the wall position. Nevertheless, we have checked that the black curves in Fig. 3 are almost coincident with the ones in Fig. 8.

7 Conclusions

This work is the second of a series in which we aim to derive the equation of motion of a bubble wall, as well as the wall profile, under the most general conditions. In Ref. [30],

⁷On the other hand, the approximation $\rho_w = \tilde{R}$ and the analytic approximation for $r_w(t)$ given in footnote 6 have an error of approximately 2.5% for the case in the left panel of Fig. 8 and 17% for the case in the right panel. The corresponding curves are halfway between the LO and NNLO results of Fig. 8.

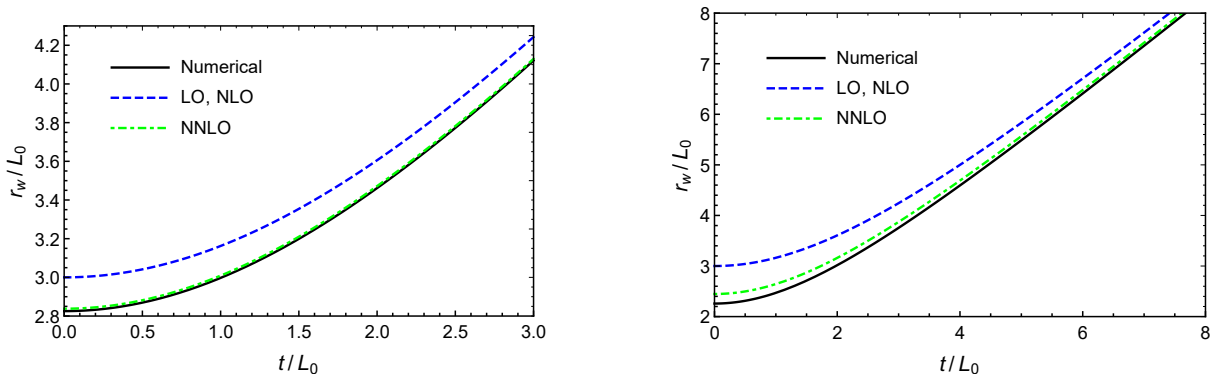


Figure 8: The bubble radius and its approximations for the two potential shapes shown in Fig. 1 (cf. Fig. 3).

we considered an infinitely thin wall of arbitrary shape in a vacuum phase transition, and in a forthcoming paper we will consider a thermal phase transition. However, the usual thin-wall approximation breaks down if the worldvolume bends in such a way that the curvature radius becomes of the order of the wall width (which may happen, in particular, for an accelerated planar or spherical wall). In this paper, we have presented a method to obtain the wall profile and the wall EOM perturbatively in the wall width. For simplicity, we have considered a vacuum phase transition, but the generalization is straightforward.

The usual thin-wall approximation assumes a bubble profile of the form $\phi = \phi(n)$, where n is the distance perpendicular to the wall hypersurface. In a coordinate system where this variable is a coordinate, such a rigid profile has a fixed width l and a constant surface tension σ . Assuming also that quantities such as the metric vary little across the thin wall, one obtains an EOM for the wall surface which depends on the ratio $\Delta V/\sigma$. Assuming that the potential is almost degenerate, one also obtains an estimation for the parameter σ . In Ref. [30], we showed that all the above remains valid at next-to-leading order in the wall width, and we calculated the corrections to the LO profile $\phi_0(n)$ and surface tension σ_0 . In the present paper, we have derived a systematic calculation of the field profile and the wall EOM at higher orders in the wall width. As we have seen, at the next-to-next-to-leading order, ϕ no longer depends solely on n . Thus, the corrections to the quantity σ are no longer constant. Besides, new parameters appear in the wall EOM, such as the wall width l . This quantity, which we concretely define as the root mean square value of n weighted with the function $(\partial_n \phi)^2$, also varies along the hypersurface beyond the next-to-leading order.

To summarize our method, we first write the field equation in normal Gaussian coordinates n, ξ^a . Thus, the zeroth-thickness approximation corresponds to 1) neglecting the dependence of ϕ on ξ^a , 2) neglecting the mean curvature of the hypersurface $K|_0$ as well as the variation of the quantity K with n , and 3) approximating the potential V by a degenerate potential V_0 . Then, we essentially consider the equation for ϕ as an expansion in $K, V - V_0$, and the successive derivatives $\partial_a \phi, \partial_n K$. This procedure gives simple equations for ϕ at each order, which can be easily solved. All these equations have the same form beyond the leading order, and we found their general solution. Each correction to ϕ is given by a combination of terms of the form $f(n)\partial_n^k K(\xi^a)$ and can be readily put in a covariant form. On the other hand, integrating the field equation with respect to n gives the wall EOM at each order. The LO and NLO equations are of the form $\sigma K = \Delta V$,

while at higher orders there are also terms with derivatives $\partial_n^k K$.

Small modifications of this treatment can be convenient for certain cases. As an example, we have considered the O(3,1)-symmetric bubble or the corresponding O(4)-symmetric instanton. The symmetry of the problem makes it convenient to replace the coordinates n, ξ^a with a single variable $\rho = \sqrt{r^2 - t^2}$. This approach is a direct generalization of Coleman's treatment [32] and gives the finite-width corrections to the nucleation radius.

For a simple case such as that of a spherical bubble, a numerical computation of the field profile is straightforward, and we have considered this case to test our results. As we have seen, the NNLO solution improves significantly the NLO one and gives an excellent approximation both for the profile and the wall position, even for potentials which depart significantly from the degenerate approximation. For a general wall evolution, a numerical approach such as a lattice calculation can be quite computationally intensive. On the other hand, our analytic expansion can be cumbersome, but the numerical evaluation of the expressions will generally be straightforward. In particular, for a polynomial potential, we have obtained analytic expressions for the field profile and the coefficients of the EOM. For a planar wall with small deformations, we have obtained analytic solutions for the evolution of the perturbations beyond the zero-thickness approximation.

Acknowledgements

This work was supported by Universidad Nacional de Mar del Plata, grant EXA1091/22.

A Normal Gaussian coordinates

In this appendix we review the construction and properties of normal Gaussian coordinates and the extrinsic curvature tensor of a hypersurface (for details, see, e.g., [31, 46, 47]).

Given a point $X^\mu(\xi^a)$ on the hypersurface Σ and the normal vector N^μ , let us consider a geodesic that crosses Σ perpendicularly. The general equation for a geodesic is

$$\frac{d^2 x^\mu}{dn^2} + \Gamma_{\nu\rho}^\mu \frac{dx^\nu}{dn} \frac{dx^\rho}{dn} = 0, \quad (117)$$

where n is an arbitrary parameter and $\Gamma_{\alpha\beta}^\mu = \frac{1}{2}g^{\mu\nu}(\frac{\partial g_{\nu\alpha}}{\partial x^\beta} + \frac{\partial g_{\nu\beta}}{\partial x^\alpha} - \frac{\partial g_{\alpha\beta}}{\partial x^\nu})$ are the Christoffel symbols. In our case, we have the initial conditions

$$x^\mu(0) = X^\mu(\xi^a), \quad \frac{dx^\mu}{dn}(0) = N^\mu(\xi^a), \quad (118)$$

and n becomes the proper distance. Indeed, Eq. (117) has the first integral

$$g_{\mu\nu} \frac{dx^\nu}{dn} \frac{dx^\mu}{dn} = -1, \quad (119)$$

where the specific value of the constant comes from the second condition (118) and the normalization of N^μ . As a consequence, the line element on the geodesic is given by $ds^2 = g_{\mu\nu} dx^\mu dx^\nu = -dn^2$. According to Eq. (119), in the coordinates $\bar{x}^\mu = (\xi^a, n)$ we have $\bar{g}_{nn} = -1$ along the geodesic. Near Σ , the change of coordinates is given by Eq. (5),

which implies that $\bar{g}_{an}|_{n=0} = g_{\mu\nu}\partial_a X^\nu N^\mu = 0$. Moreover, \bar{g}_{an} is constant along the geodesic. This can be seen from the fact that, in normal Gaussian coordinates, Eq. (117) takes the form $\bar{\Gamma}_{nn}^\mu = 0$, which implies $\partial_n \bar{g}_{an} = 0$. Hence, we have $\bar{g}_{an} = 0$ also away from Σ . The inverse matrix $\bar{g}^{\mu\nu}$ also fulfills $\bar{g}^{nn} = -1$, $\bar{g}^{an} = 0$, and we have $\bar{g}^{ac}\bar{g}_{cb} = \delta_b^a$. It is easy to verify that the Christoffel symbols are given by Eq. (6).

We define the vector field

$$n^\mu = dx^\mu/dn, \quad (120)$$

which is tangent to the geodesics and coincides with N^μ on Σ . According to Eq. (119), it satisfies $n_\mu n^\mu = -1$ everywhere. Furthermore, the property $\bar{g}_{an} = 0$ implies that we have $\partial_a x^\mu n_\mu = 0$ everywhere. These properties indicate that n^μ is a normal vector to the surfaces Σ_n of $n = \text{constant}$. In normal Gaussian coordinates we have

$$\bar{n}^\mu = (0, 0, 0, 1), \quad \bar{n}_\mu = (0, 0, 0, -1). \quad (121)$$

We may write the latter covariantly as $n_\mu = -\partial_\mu n$. The vector $N_\mu = -\partial_\mu F/s$ coincides with n_μ only at $n = 0$, i.e., on Σ . Since both vectors are normalized, we have $N^\nu \nabla_\mu N_\nu = 0$ and $n^\nu \nabla_\mu n_\nu = 0$. On the other hand, n^μ also satisfies $n^\mu \nabla_\mu n_\nu = 0$, as can be easily seen from Eqs. (121) and (6).

To obtain the expression for n as a function of x^μ , we begin by considering the expansion $F = an + bn^2 + cn^3 + \dots$, where $a = \partial_n F|_{n=0}$, $b = \frac{1}{2}\partial_n^2 F|_{n=0}$, and so on. The inverse of this expansion is

$$n = F/a - (b/a)(F/a)^2 + [2(b/a)^2 - c/a](F/a)^3 + \dots \quad (122)$$

Taking into account that $\partial_n F = n^\mu \partial_\mu F = -sn^\mu N_\mu$ and similar equations for successive derivatives, then evaluating at $n = 0$, we obtain

$$a = s|_{n=0}, \quad b = \frac{1}{2}N^\nu \partial_\nu s|_{n=0}, \quad c = \frac{1}{6}[N^\rho N^\nu \nabla_\rho \partial_\nu s - sN^\rho N^\mu N^\nu \nabla_\rho \nabla_\nu N_\mu]|_{n=0}. \quad (123)$$

Inserting the coefficients (123) in Eq. (122), we obtain

$$n = c_1(\xi^a, 0)F + c_2(\xi^a, 0)F^2 + c_3(\xi^a, 0)F^3 + \dots, \quad (124)$$

with

$$c_1 = \frac{1}{s}, \quad c_2 = -\frac{N^\nu \partial_\nu s}{2s^3}, \quad c_3 = \frac{(N^\nu \partial_\nu s)^2}{2s^5} + \frac{N^\rho N^\nu N^\mu \nabla_\rho \nabla_\nu (sN_\mu)}{6s^4}. \quad (125)$$

The expression (124) gives an expansion with coefficients evaluated at the hypersurface Σ . To obtain n as a function of the coordinates x^μ , we may expand these coefficients as

$$c_i(\xi^a, 0) = c_i(\xi^a, n) - \partial_n c_i(\xi^a, n)n + \frac{1}{2}\partial_n^2 c_i(\xi^a, n)n^2 + \mathcal{O}(n^2). \quad (126)$$

Using $\partial_n c_i = N^\alpha \partial_\alpha c_i$, inserting Eq. (126) in Eq. (124), and using the latter recursively, we obtain Eq. (7). Notice that, although Eq. (7) looks very similar to the expansion (124)-(125), there is a sign difference in the quadratic term. Besides, all the quantities in Eq. (7) are evaluated at the point x^μ and can be obtained from $F(x^\mu)$ using $s^2 = -F_{,\alpha}F^{,\alpha}$, $sN_\mu = -\partial_\mu F$, and $\partial_\nu s = N^\mu \nabla_\nu \partial_\mu F$.

We define the extrinsic curvature tensor of the hypersurfaces Σ_n as [47]

$$K_{\mu\nu} = -\nabla_\mu n_\nu. \quad (127)$$

From Eq. (121), we readily see that, in normal Gaussian coordinates, we have

$$\bar{K}_{n\mu} = 0, \quad \bar{K}_{ab} = -\bar{\Gamma}_{ab}^n \quad (128)$$

and, hence, this tensor has the properties $n^\nu K_{\mu\nu} = 0$, $K_{\mu\nu} = K_{\nu\mu}$. We are interested in the mean curvature $K = \bar{g}^{ab} \bar{K}_{ab} = g^{\mu\nu} K_{\mu\nu}$ and its derivatives with respect to n . Applying the general equation $\nabla_\rho \nabla_\nu A_\mu - \nabla_\nu \nabla_\rho A_\mu = R^\sigma{}_{\mu\rho\nu} A_\sigma = 0$ (in flat space) to $A_\mu = n_\mu$, we obtain the equality $\nabla_\rho K_{\mu\nu} = \nabla_\mu K_{\rho\nu}$. Using this property in the covariant derivative of $n^\mu K_{\mu\nu} = 0$, we obtain

$$n^\mu \nabla_\mu K_{\rho\nu} = K_\rho{}^\mu K_{\mu\nu}. \quad (129)$$

Taking into account that $n^\nu \nabla_\nu K = \partial_n K$ and repeating the manipulations for the second derivative, we obtain the equations

$$\partial_n K = K^{\mu\nu} K_{\mu\nu}, \quad \partial_n^2 K = 2K^\mu{}_\nu K^\nu{}_\rho K^\rho{}_\mu. \quad (130)$$

At $n = 0$, we can write these expressions in terms of N_μ . For that aim, we notice that, due to the property $n^\mu K_{\mu\nu} = n^\mu K_{\nu\mu} = 0$, we can use the projector $P_\mu{}^\nu = \delta_\mu^\nu + n_\mu n^\nu$ to write Eq. (127) in the form $K_{\mu\nu} = -P_\mu{}^\rho P_\nu{}^\sigma \nabla_\rho n_\sigma$. Due to the tangential projections, it doesn't matter how the vector n^μ is extended out of Σ , and we can replace it with N^μ . Hence we obtain $K_{\mu\nu} = -h_\mu{}^\rho h_\nu{}^\sigma \nabla_\rho N_\sigma$, with $h_\mu{}^\nu = (\delta_\mu^\nu + N_\mu N^\nu)$. Furthermore, since our vector N_μ keeps the normalization $N_\mu N^\mu = -1$ even out of Σ , we have $N^\sigma \nabla_\rho N_\sigma = 0$ and we obtain Eq. (9). Inserting the latter in Eqs. (8) and (130), we obtain Eqs. (11)⁸.

B Wall profile and EOM parameters

The calculation of the NNLO field profile, and, hence, of parameters such as the surface tension, involves several functions of n and integrals with respect to this variable. We shall now see that these equations become simpler if we use as a variable the LO field ϕ_0 . This can be accomplished through the function $n(\phi_0)$ defined by Eqs. (25)-(26). For instance, it is well known that the LO surface tension can be written as

$$\sigma_0 = \int_{a_+}^{a_-} \phi_h(\phi_0) d\phi_0, \quad (131)$$

where ϕ_h is the function defined in Eq. (24). This expression can be readily obtained from $\sigma_0 = \int_{-\infty}^{+\infty} (\partial_n \phi_0)^2 dn$ using $d\phi_0/dn = -\phi_h$ and $dn = -d\phi_0/\phi_h(\phi_0)$. The advantage of Eq. (131) is that it gives σ_0 directly from the degenerate potential $V_0(\phi)$ without going through with profile $\phi_0(n)$.

Using the same change of variables, we can obtain all the quantities appearing in the perturbative calculation as integrals involving the functions $\phi_h(\phi)$ and $\tilde{V}(\phi)$. In particular, from the first of Eqs. (35) we obtain the LO values of some quantities,

$$I_0^{(0)} = \int_{a_+}^{\phi_0} \phi_h(\phi) d\phi, \quad I_0^{(1)} = \int_{a_+}^{\phi_0} \phi_h(\phi) n(\phi) d\phi, \quad \mu_0 = \int_{a_+}^{a_-} \phi_h(\phi) n(\phi)^2 d\phi. \quad (132)$$

⁸It is worth remarking that, although $K_{\mu\nu} = -\nabla_\mu n_\nu$ is symmetric, $\nabla_\mu N_\nu$ is not, and we have $K_{\mu\nu} = -\nabla_\mu N_\nu - N_\mu N^\alpha \nabla_\alpha N_\nu$. Thus, using either $K^{\mu\nu} K_{\mu\nu}$ or $K^{\mu\nu} K_{\nu\mu}$, we obtain two different expressions for $\partial_n K$, namely, $\partial_n K = \nabla^\mu N^\nu \nabla_\mu N_\nu + N^\alpha N^\beta \nabla_\beta N^\nu \nabla_\alpha N_\nu$ or $\partial_n K = \nabla^\mu N^\nu \nabla_\nu N_\mu$.

The first of these functions appears in the function f_1 , Eq. (37). Using Eq. (51), we have

$$f_1(\phi_0) = \tilde{V}(\phi_0) - \tilde{V}(a_+) + (\Delta V_1/\sigma_0)I_0^{(0)}(\phi_0). \quad (133)$$

Using this equation in Eq. (44) and the latter in Eqs. (43) and (45), we obtain the quantities

$$C_1(\phi_0) = \int_{\phi_*}^{\phi_0} \frac{f_1(\phi)}{\phi_h(\phi)^3} d\phi, \quad c_1 = 2\sigma_0^{-1} \int_{a_+}^{a_-} C_1(\phi) [V_0'(\phi)n(\phi) - \phi_h(\phi)] d\phi. \quad (134)$$

and the first correction to the profile, $\phi_1(\phi_0) = \phi_h(\phi_0)[C_1(\phi_0) + c_1]$. Both ϕ_h and f_1 vanish at $\phi_0 = a_{\pm}$ (corresponding to $n = \pm\infty$). In these limits, ϕ_1 takes the values

$$\phi_{1\pm} = -\frac{\tilde{V}'(a_{\pm})}{V_0''(a_{\pm})} = -\frac{V'(a_{\pm})}{V_0''(a_{\pm})}, \quad (135)$$

and it can be seen that we have $\partial_n \phi_1 \rightarrow 0$.

From the second of Eqs. (35), we obtain the NLO integrals

$$I_1^{(0)}(\phi_0) = \phi_h(\phi_0)\phi_1(\phi_0) + \int_{a_+}^{\phi_0} \frac{f_1(\phi) d\phi}{\phi_h(\phi)}, \quad \sigma_1 = \int_{a_+}^{a_-} \frac{f_1(\phi)}{\phi_h(\phi)} d\phi, \quad (136)$$

where we have used Eq. (36), and Eq. (63) gives

$$\mu_1 = \int_{a_+}^{a_-} \frac{f_1(\phi)}{\phi_h(\phi)} n(\phi)^2 d\phi + 2 \int_{a_+}^{a_-} \phi_h(\phi) C_1(\phi) n(\phi) d\phi. \quad (137)$$

Taking into account Eqs. (40), (41), and (36), the function \tilde{f}_2 , Eq. (38), is given by

$$\tilde{f}_2 = \tilde{V}'(\phi_0)\phi_1 + \frac{1}{2}V_0''(\phi_0)\phi_1^2 - \frac{[f_1 + V_0'(\phi_0)\phi_1]^2}{2\phi_h^2} + \frac{\Delta V_1}{\sigma_0}I_1^{(0)} + \left[\frac{\Delta V_2}{\sigma_0} - \frac{\Delta V_1\sigma_1}{\sigma_0^2} \right] I_0^{(0)} - V_{2+}. \quad (138)$$

Using these equations in Eqs. (48)-(49), we obtain the quantities

$$C_{2a}(\phi_0) = \int_{\phi_*}^{\phi_0} \frac{\tilde{f}_2(\phi)}{\phi_h(\phi)^3} d\phi, \quad C_{2b}(\phi_0) = - \int_{\phi_*}^{\phi_0} \frac{I_0^{(1)}(\phi)}{\phi_h(\phi)^3} d\phi, \quad (139)$$

$$c_{2a} = \sigma_0^{-1} \int_{a_+}^{a_-} \left\{ 2[V_0'(\phi)n(\phi) - \phi_h(\phi)] C_{2a}(\phi) - [f_1(\phi) + V_0'(\phi)\phi_1(\phi)]^2 \frac{n(\phi)}{\phi_h(\phi)^3} \right\} d\phi, \quad (140)$$

$$c_{2b} = 2\sigma_0^{-1} \int_{a_+}^{a_-} [V_0'(\phi)n(\phi) - \phi_h(\phi)] C_{2b}(\phi) d\phi \quad (141)$$

and the second correction to the profile, $\phi_2 = \phi_{2a} + \phi_{2b}\partial_n K_0$, with

$$\phi_{2a}(\phi_0) = \phi_h(\phi_0) [C_{2a}(\phi_0) + c_{2a}], \quad \phi_{2b}(\phi_0) = \phi_h(\phi_0) [C_{2b}(\phi_0) + c_{2b}]. \quad (142)$$

At $\phi_0 = a_{\pm}$ (i.e., $n = \pm\infty$), ϕ_2 takes the values

$$\phi_{2\pm} = -\frac{\tilde{V}''(a_{\pm})\phi_{1\pm} + \frac{1}{2}V_0'''(a_{\pm})\phi_{1\pm}^2}{V_0''(a_{\pm})}. \quad (143)$$

We can also write Eqs. (54) and (64) as

$$\tilde{\sigma}_2 = \int_{a_+}^{a_-} \left[\frac{[f_1(\phi) + V_0'(\phi)\phi_1(\phi)]^2}{\phi_h^2(\phi)} + \tilde{f}_2(\phi) \right] \frac{d\phi}{\phi_h(\phi)}. \quad (144)$$

$$\tilde{\mu}_2 = \int_{a_+}^{a_-} \left\{ \left[\frac{[f_1(\phi) + V_0'(\phi)\phi_1(\phi)]^2}{\phi_h^3(\phi)} + \frac{\tilde{f}_2(\phi)}{\phi_h(\phi)} \right] n(\phi)^2 + 2\phi_h(\phi)C_{2a}(\phi)n(\phi) \right\} d\phi, \quad (145)$$

$$\alpha = \int_{a_+}^{a_-} \phi_h(\phi) \left[2C_{2b}(\phi)n(\phi) - \frac{1}{3}n(\phi)^4 \right] d\phi. \quad (146)$$

Let us now consider the potential V_0 of Eq. (95) and the linear $\tilde{V} = c\phi$. We begin by calculating the LO field profile $\phi_0(n)$ from Eqs. (24)-(26). The result does not depend on the integration constant ϕ_* , and we shall take $\phi_* = (a_+ + a_-)/2$ to take advantage of the symmetry of V_0 . We also define the parameter $a = (a_- - a_+)/2$ and we make the changes of variables $x = (\phi - \phi_*)/a$, $x_0 = (\phi_0 - \phi_*)/a$ in the integrals in Eqs. (25)-(26). Since the integration range of ϕ and ϕ_0 is the interval $[a_+, a_-]$, the variables x and x_0 vary between -1 and $+1$. Thus, the function ϕ_h is given by $\phi_h = \sqrt{\lambda/2}a^2(1 - x_0^2)$. After this change of variable in Eq. (25), it is apparent by symmetry that $n_* = 0$, and we obtain

$$n = -\frac{a^{-1}}{\sqrt{2\lambda}} \log \left(\frac{1 - x_0}{1 + x_0} \right). \quad (147)$$

Inverting this expression, we obtain $x_0 = -\tanh(\sqrt{\lambda/2}an)$.

The LO quantities (131)-(132) give $\sigma_0 = \frac{4}{3}\sqrt{\lambda/2}a^3$, $\mu_0 = \frac{\pi^2-6}{9}\sqrt{2/\lambda}a$,

$$I_0^0(x_0) = a^3\sqrt{\lambda/2} (2/3 + x_0 - x_0^3/3), \quad (148)$$

$$I_0^1(x_0) = \frac{1}{6}a^2 \left[x_0^2 - 1 + x_0(x_0^2 - 3) \log \left(\frac{1 + x_0}{1 - x_0} \right) - 2 \log \left(\frac{1 - x_0^2}{4} \right) \right]. \quad (149)$$

For $\tilde{V} = c\phi$, Eq. (30) gives $\Delta V_1 = -2ca$, and we obtain $f_1 = -(ca/2)x_0(1 - x_0^2)$ and $\phi_1 = -c/(2a^2\lambda)$. In this case, we have $V_0''(a_+) = V_0''(a_-)$ and the derivative V' is a constant. As a consequence, Eq. (30) gives $\Delta V_2 = 0$, and we obtain

$$\tilde{f}_2(x_0) = \frac{3c^2}{8\lambda a^2}(x_0^2 - 1), \quad C_{2a}(x_0) = \frac{3\sqrt{2}c^2}{16\lambda^{5/2}a^7} \left[\frac{2x_0}{x_0^2 - 1} - \log \left(\frac{1 + x_0}{1 - x_0} \right) \right], \quad (150)$$

and

$$\begin{aligned} C_{2b}(x_0) = & -\frac{\sqrt{2}a^{-3}}{48\lambda^{3/2}} \left\{ \frac{4x_0}{(1 - x_0^2)^2} [(1 - 6\log 2)x_0^2 + 10\log 2 - 1] \right. \\ & - 2\log(1 - x_0) \left[\frac{x_0(5x_0 + 4) - 3}{(1 + x_0)^2} + 3\log 2 \right] + 2\log(1 + x_0) \left[\frac{x_0(5x_0 - 4) - 3}{(1 - x_0)^2} + 3\log 2 \right] \\ & \left. + 3\log^2(1 - x_0) - 3\log^2(1 + x_0) + 6\text{Li}_2 \left(\frac{1 + x_0}{2} \right) - 6\text{Li}_2 \left(\frac{1 - x_0}{2} \right) \right\}, \quad (151) \end{aligned}$$

where $\text{Li}_2(z) = \sum_{k=1}^{\infty} z^k/k^2 = -\int_0^z \log(1-t)dt/t$ is the dilogarithm function [48]. The integrals (140)-(141) give $c_{2a} = c_{2b} = 0$ since their integrands are odd after the change of

variables. The first term in the integrands of (144)-(145) vanishes in this case, which is more easily seen in the expressions (35), and we obtain

$$\tilde{\sigma}_2 = -\frac{3\sqrt{2}}{4\lambda^{3/2}} \frac{c^2}{a^3}, \quad \tilde{\mu}_2 = -\frac{\sqrt{2}(\pi^2 - 6)}{24\lambda^{5/2}} \frac{c^2}{a^5}, \quad \alpha = 0.346305 \frac{(2/\lambda)^{3/2}}{3a}. \quad (152)$$

Thus, for instance, Eq. (62) gives

$$\frac{\sigma}{\sigma_0} = 1 - \frac{9c^2}{8\lambda^2 a^6} - \left(\frac{\pi^2}{6} - 1\right) \frac{\partial_n K_0|_0}{\lambda a^2}. \quad (153)$$

References

- [1] C. J. Hogan, *Gravitational radiation from cosmological phase transitions*, *Mon. Not. Roy. Astron. Soc.* **218** (1986) 629–636.
- [2] M. S. Turner and F. Wilczek, *Relic gravitational waves and extended inflation*, *Phys. Rev. Lett.* **65** (1990) 3080–3083.
- [3] A. Kosowsky, M. S. Turner and R. Watkins, *Gravitational waves from first order cosmological phase transitions*, *Phys. Rev. Lett.* **69** (1992) 2026–2029.
- [4] M. Kamionkowski, A. Kosowsky and M. S. Turner, *Gravitational radiation from first order phase transitions*, *Phys. Rev. D* **49** (1994) 2837–2851, [astro-ph/9310044].
- [5] V. Kuzmin, V. Rubakov and M. Shaposhnikov, *On the Anomalous Electroweak Baryon Number Nonconservation in the Early Universe*, *Phys. Lett. B* **155** (1985) 36.
- [6] A. G. Cohen, D. Kaplan and A. Nelson, *Progress in electroweak baryogenesis*, *Ann. Rev. Nucl. Part. Sci.* **43** (1993) 27–70, [hep-ph/9302210].
- [7] A. Vilenkin and E. P. S. Shellard, *Cosmic Strings and Other Topological Defects*. Cambridge University Press, 7, 2000.
- [8] L. M. Widrow, *Dynamics of Thick Domain Walls*, *Phys. Rev. D* **40** (1989) 1002.
- [9] L. M. Widrow, *The Collapse of Nearly Spherical Domain Walls*, *Phys. Rev. D* **39** (1989) 3576.
- [10] R. Gregory, D. Haws and D. Garfinkle, *The Dynamics of Domain Walls and Strings*, *Phys. Rev. D* **42** (1990) 343–348.
- [11] D. Garfinkle and R. Gregory, *Corrections to the Thin Wall Approximation in General Relativity*, *Phys. Rev. D* **41** (1990) 1889.
- [12] R. Gregory, *Effective actions for bosonic topological defects*, *Phys. Rev. D* **43** (1991) 520–525.
- [13] V. Silveira and M. D. Maia, *Topological defects and corrections to the Nambu action*, *Phys. Lett. A* **174** (1993) 280–284, [gr-qc/9303017].

- [14] A. L. Larsen, *Comment on thickness corrections to Nambu wall*, *Phys. Lett. A* **181** (1993) 369–372, [[hep-th/9306046](#)].
- [15] B. Carter and R. Gregory, *Curvature corrections to dynamics of domain walls*, *Phys. Rev. D* **51** (1995) 5839–5846, [[hep-th/9410095](#)].
- [16] H. Arodz and A. L. Larsen, *On dynamics of cylindrical and spherical relativistic domain walls of finite thickness*, *Phys. Rev. D* **49** (1994) 4154–4166, [[hep-th/9309089](#)].
- [17] H. Arodz, *On expansion in the width for domain walls*, *Nucl. Phys. B* **450** (1995) 174–188, [[hep-th/9502018](#)].
- [18] H. Arodz, *Thick domain walls in a polynomial approximation*, *Phys. Rev. D* **52** (1995) 1082–1095, [[hep-th/9501073](#)].
- [19] H. Arodz, *Expansion in the width and collective dynamics of a domain wall*, *Nucl. Phys. B* **509** (1998) 273–293, [[hep-th/9703168](#)].
- [20] L. Leitao and A. Megevand, *Spherical and non-spherical bubbles in cosmological phase transitions*, *Nucl. Phys. B* **844** (2011) 450–470, [[1010.2134](#)].
- [21] J. Garriga and A. Vilenkin, *Perturbations on domain walls and strings: A Covariant theory*, *Phys. Rev. D* **44** (1991) 1007–1014.
- [22] F. C. Adams, K. Freese and L. M. Widrow, *Evolution of Nonspherical Bubbles*, *Phys. Rev. D* **41** (1990) 347.
- [23] B. Link, *Deflagration instability in the quark - hadron phase transition*, *Phys. Rev. Lett.* **68** (1992) 2425–2428.
- [24] P. Y. Huet, K. Kajantie, R. G. Leigh, B.-H. Liu and L. D. McLerran, *Hydrodynamic stability analysis of burning bubbles in electroweak theory and in QCD*, *Phys. Rev.* **D48** (1993) 2477–2492, [[hep-ph/9212224](#)].
- [25] A. Megevand and F. A. Membiela, *Stability of cosmological deflagration fronts*, *Phys. Rev.* **D89** (2014) 103507, [[1311.2453](#)].
- [26] A. Megevand and F. A. Membiela, *Stability of cosmological detonation fronts*, *Phys. Rev. D* **89** (2014) 103503, [[1402.5791](#)].
- [27] J. Braden, J. R. Bond and L. Mersini-Houghton, *Cosmic bubble and domain wall instabilities I: parametric amplification of linear fluctuations*, *JCAP* **03** (2015) 007, [[1412.5591](#)].
- [28] J. Braden, J. R. Bond and L. Mersini-Houghton, *Cosmic bubble and domain wall instabilities II: Fracturing of colliding walls*, *JCAP* **08** (2015) 048, [[1505.01857](#)].
- [29] J. R. Bond, J. Braden and L. Mersini-Houghton, *Cosmic bubble and domain wall instabilities III: The role of oscillons in three-dimensional bubble collisions*, *JCAP* **09** (2015) 004, [[1505.02162](#)].

- [30] A. Mégevand and F. A. Membiela, *Thin and thick bubble walls. Part I. Vacuum phase transitions*, *JCAP* **06** (2023) 007, [2302.13349].
- [31] S. Carroll, *Spacetime and Geometry: An Introduction to General Relativity*. Pearson Education Limited, 2014.
- [32] S. R. Coleman, *The Fate of the False Vacuum. 1. Semiclassical Theory*, *Phys. Rev. D* **15** (1977) 2929–2936.
- [33] M. Spivak, *A comprehensive introduction to differential geometry*, vol. Vol.3. Publish or Perish, 3rd ed., 1999.
- [34] M. Spivak, *A comprehensive introduction to differential geometry*, vol. Vol.4. Publish or Perish, 3rd ed., 1999.
- [35] S. K. Blau, E. I. Guendelman and A. H. Guth, *The Dynamics of False Vacuum Bubbles*, *Phys. Rev. D* **35** (1987) 1747.
- [36] A. Aurilia, M. Palmer and E. Spallucci, *Evolution of Bubbles in a Vacuum*, *Phys. Rev. D* **40** (1989) 2511.
- [37] A. Aguirre and M. C. Johnson, *Dynamics and instability of false vacuum bubbles*, *Phys. Rev. D* **72** (2005) 103525, [gr-qc/0508093].
- [38] B.-H. Lee, C. H. Lee, W. Lee, S. Nam and C. Park, *Dynamics of false vacuum bubbles with the negative tension due to nonminimal coupling*, *Phys. Rev. D* **77** (2008) 063502, [0710.4599].
- [39] K.-W. Ng and S.-Y. Wang, *Collapse of Vacuum Bubbles in a Vacuum*, *Phys. Rev. D* **83** (2011) 043512, [1006.3441].
- [40] M. Gleiser, E. W. Kolb and R. Watkins, *Phase transitions with subcritical bubbles*, *Nucl. Phys. B* **364** (1991) 411–450.
- [41] G. Gelmini and M. Gleiser, *Kinetics of subcritical bubbles and the electroweak transition*, *Nucl. Phys. B* **419** (1994) 129–146, [hep-ph/9211303].
- [42] M. Gleiser, A. F. Heckler and E. W. Kolb, *Modeling thermal fluctuations: Phase mixing and percolation*, *Phys. Lett. B* **405** (1997) 121–125, [cond-mat/9512032].
- [43] E. Witten, *Cosmic Separation of Phases*, *Phys. Rev. D* **30** (1984) 272–285.
- [44] M. Gleiser and R. Roberts, *Gravitational waves from collapsing vacuum domains*, *Phys. Rev. Lett.* **81** (1998) 5497–5500, [astro-ph/9807260].
- [45] P. Burda, R. Gregory and I. Moss, *The fate of the Higgs vacuum*, *JHEP* **06** (2016) 025, [1601.02152].
- [46] J. Synge, *Relativity: The General Theory*. North-Holland series in physics. North-Holland Publishing Company, 1960.
- [47] R. M. Wald, *General Relativity*. Chicago Univ. Pr., Chicago, USA, 1984, 10.7208/chicago/9780226870373.001.0001.

- [48] I. A. S. Milton Abramowitz, *Handbook of Mathematical Functions with Formulas, Graphs, and Mathematical Table*. Dover Publications, 1970.